Neuron

Mitochondrial cannabinoid receptors gate corticosterone impact on novel object recognition

--Manuscript Draft--

Manuscript Number:	NEURON-D-22-00573R3
Full Title:	Mitochondrial cannabinoid receptors gate corticosterone impact on novel object recognition
Article Type:	Report
Keywords:	Corticosterone, object recognition memory, endocannabinoids, mitochondrial CB1 receptor, mitochondrial calcium, retrieval, consolidation, hippocampus, locus coeruleus, GABA, noradrenaline
Corresponding Author:	Giovanni Marsicano Bordeaux, FRANCE
First Author:	Urszula Skupio
Order of Authors:	Urszula Skupio
	Julia Welte
	Roman Serrat
	Abel Eraso-Pichot
	Francisca Julio-Kalajzić
	Doriane Gisquet
	Astrid Cannich
	Sebastien Delcasso
	Isabelle Matias
	Unai B Fundazuri
	Sandrine Pouvreau
	Antonio C. Pagano Zottola
	Gianluca Lavanco
	Inigo Ruiz de Azua
	Beat Lutz
	Luigi Bellocchio
	Arnau Busquets-Garcia
	Francis Chaouloff
	Giovanni Marsicano
Abstract:	SUMMARY Corticosteroid-mediated stress responses require the activation of complex brain circuits involving mitochondrial activity, but the underlying cellular and molecular mechanisms are scantly known. The endocannabinoid system is implicated in stress coping and it can directly regulate brain mitochondrial functions via type-1 cannabinoid receptors (CB1) associated with mitochondria membranes (mtCB1). In this study, we show that the impairing effect of corticosterone in the novel object recognition (NOR) task in mice requires mtCB1 receptors and the regulation of mitochondrial calcium levels in neurons. Different brain circuits are modulated by this mechanism to mediate the impact of corticosterone on specific phases of the task. Thus, whereas corticosterone recruits mtCB1 receptors in noradrenergic neurons to impair NOR

	consolidation, mtCB1 receptors in local hippocampal GABAergic interneurons are required to inhibit NOR retrieval. These data reveal unforeseen mechanisms mediating the effects of corticosteroids during different phases of NOR, involving mitochondrial calcium alterations in different brain circuits.
Suggested Reviewers:	Carmen Sandi Professor of Neuroscience, EPFL: Ecole Polytechnique Federale de Lausanne carmen.sandi@epfl.ch Dr Sandi is a specialist in the fields of stress and bioenergetics.
	Matthew Hill mnhill@ucalgary.ca Expert in stress and endocannabinoids
	Martin Picard mp3484@cumc.columbia.edu Expert in mitochondria and brain functions
	Tamas Horvath Expert in brian bioenergetics
	Jaime Dejuansanz jaime.dejuansanz@icm-institute.org Expert in brain mitochondrial functions
Opposed Reviewers:	Vincenzo Di Marzo Potential conflict of interest
	Mauro Maccarrone Potential Conflict of interest
	Zsolt Lenkei Potential conflict of interest
Additional Information:	
Question	**Response**
Standardized datasets A list of datatypes considered standardized under Cell Press policy is available here. Does this manuscript report new standardized datasets?	No
Original Code<p>Does this manuscript report original code?	No
If your paper is accepted, we encourage you to publish the original, unprocessed data alongside your Cell Press paper through Mendeley Data. For more information, please refer to our detailed instructions.	I do not wish to publish my original data.

Giovanni Marsicano, DVM, PhD
Deputy Director
NeuroCentre Magendie,
INSERM U1215 Université Bordeaux
Group Leader
Endocannabinoids and Neuroadaptation

146 rue Léo-Saignat
33077 Bordeaux Cedex- France
Tel: +33 (0)5 5757 3756
Fax:+33 (0)5 5757 3669
giovanni.marsicano@inserm.fr

Bordeaux, 30 March 2023

Dear Dr. Schridde, dear Uli,

I apologize again for the previous hurried submission of an incompletely revised version of our manuscript NEURON-D-22-00573R2, "Mitochondrial cannabinoid receptors gate corticosterone impact on novel object recognition" by Skupio et al.

We now carefully addressed all the Editorial concerns and we hope that everything is correctly arranged. Please find in attachment a point-by-point answer to your remarks.

I hope that the manuscript is now fitting with the required standards of *Neuron*. Thank you again for your help and understanding.

Sincerely,

Giovanni Marsicano, DVM, PhD

Editorial:

- Just to clarify: Currently highlights 2 and 3 read 2) 'MtCB1 in locus coeruleus noradrenergic cells mediates consolidation impairment' and 3) 'MtCB1 in hippocampal GABAergic neurons mediates consolidation impairment'. While the abstract states: '…Thus, whereas corticosterone recruits $mtCB_1$ receptors in noradrenergic neurons to impair NOR consolidation, $mtCB_1$ receptors in local hippocampal GABAergic interneurons are required to inhibit NOR retrieval….'. So, shouldn't the 3rd highlight mention inhibition of retrieval instead of consolidation impairment?

Thank you for pointing out this mistake, due to a silly copy & paste maneuver. We have changed the highlights to reflect accurately our findings.

Production Requirements:

- Please remove supplemental figure and table titles/legends from the main text file. à please see also below for suggestion about suppl. tables 1 and 2. If you decide to combine those and provide a separate Excel file, the title of the file should be part of the main text.
- All supplemental figures should have clear overarching descriptive titles distinct from any legend (Figure S1. Descriptive title, related to Figure 1)
- Please ensure supplemental tables reference at least one main figure or table or the STAR Methods section. à this refers to suppl table 2. Since this one refers to the stats in the suppl .figure, as a solution, I would suggest to combine Suppl. tables 1 and 2 into one large table and that the references to the main and suppl. figures. Please note that in that case the figure likely exceeds 3 pages and would need to be submitted as a separate Excel file and its title etc. have to be part of the main text, not the supplementary.

Supplemental figure legends were removed from the main text and descriptive titles were added to each figure. Tables S1 and S2 are now combined as suggested and provided as Excel file, the title of the file is provided in main text under Supplemental information titles and legends section.

- Di-form: Please insert any "declaration of interests" statements in the box on the di-form space. This exact text should also be included in the "declaration of interests" section of the manuscript. If no authors have a competing interest, please insert the text, "The authors declare no competing interests."

Appropriate statement was added to the form.

- I&D form: Please check at least one of the boxes on PAGE 4: SIGNATURE AND COMMENTS and if applicable add the respective statement in the main text.

We have agreed to add diversity statement to our manuscript and added it to the final version of the manuscript (below Declaration of interests section).

- Please remove the comments from the Highlights and eTOC document

We apologize for having overlooked this; comments were removed.

STAR Methods:

GENERAL

- STAR Methods follows a standardized structure. Please include these specific headings in the following order: RESOURCE AVAILABILITY; EXPERIMENTAL MODEL AND SUBJECT DETAILS; METHOD DETAILS; QUANTIFICATION AND STATISTICAL ANALYSIS. The list below details the information that should be reported in each section. Please see the STAR Methods guide for more information or contact me for help. --> Please use this exact structure and order and subheadings and group the respective information under the appropriate subheadings.
- Please organize this section so it is easy for the reader to appreciate the different models/experiments/analyses used. Subheadings may be used here to help organize the information (up to two levels of subheadings are permitted), but numbering is not allowed.

STAR methods section is now structured according to guidelines and follows abovementioned headings.

RESOURCE AVAILABILITY

- We require three subheadings in this section (Lead Contact, Materials Availability, and Data and Code Availability). Please be in touch if you have any questions about this and refer to the Information for Authors for specific details on Cell Press policy on reagents sharing. --> this is all good, so just as a FYI to ensure you have all three listed when reorganizing the Methods section (see previous comments)
- Cell Press now requires that published papers contain a structured "Data and Code Availability" statement within the Resource Availability section of the STAR Methods. It consists of three bulleted sections. Each section must be present. A template for the Data and Code Availability statement can be found here: https://www.cell.com/star-authors-guide. --> Please use the bulleting format and provide the respective information for each bulleting point.

- All experimental studies generate data. You must be willing to share the data reported in your paper after it is published, either through an online repository or upon request from the Lead Contact. Please revise the data portion of your availability statement accordingly. Examples of acceptable statements can be found here: https://www.cell.com/star-authors-guide. --> Please use separate bullet points for Data and Code, respectively. Also, currently you state that only the raw data will be shared upon request. However, we require all data to be shared and therefore please adjust the formulation accordingly (see also the guidelines for further details).
- To my understanding, your paper reports custom computer code. Your code must either be deposited in a repository that mints DOIs or included within the Supplemental Information before I can accept your paper. A list of repositories we endorse can be found here: https://www.cell.com/star-authors-guide. If you choose to deposit your code, please ensure it is publicly accessible and record the DOI in the Software and Algorithms section of the Key Resources Table (e.g. Zenodo will work).
- We require that the final bullet point of the Data and Code Availability statement states: "Any additional information required to reanalyze the data reported in this work paper is available from the Lead Contact upon request." Please include this statement as the final bullet point.

We introduced all abovementioned changes and details into our Resource Availability section of Methods and Key Resources Table.

EXPERIMENTAL MODEL AND SUBJECT DETAILS

- Please list here under separate headings all the experimental models (animals, human subjects, plants, microbe strains, cell lines, primary cell cultures) used in the study. For each model, provide information related to their species/strain, genotype, age/developmental stage, sex (and gender if reported for human studies), maintenance, and care, including institutional permission and oversight information for the studies the experimental animal/human study. In cases where this is appropriate, the influence (or association) of sex, gender, or both on the results of the study must be reported. --> this looks all good. But currently it's not fully clear if all animals used were male. I assume so, but please reformulate to make it clearer.

That is correct, our study only included male mice. We now stated this more clearly and provided an additional sentence explaining the reasons in the Animals paragraph of Methods section.

KEY RESOURCES TABLE

- If applicable, please include all critical software and algorithms used and generated in the Key Resources Table and include the links to download these resources in the "Identifier" column. Please note that every type of code that's not published

before or publicly available needs to be provided and reported in the Data & code section and in the KRT

Code used for analysis of our fiber photometry data was deposited on Zenodo and Key resources table was updated to include its DOI.

Additional changes not requested by the Editor:

After discussing with several lab members, we decided to provide a few more details on our fiber photometry method description, so that it's clearer and easier to replicate.

Graphical Abstract

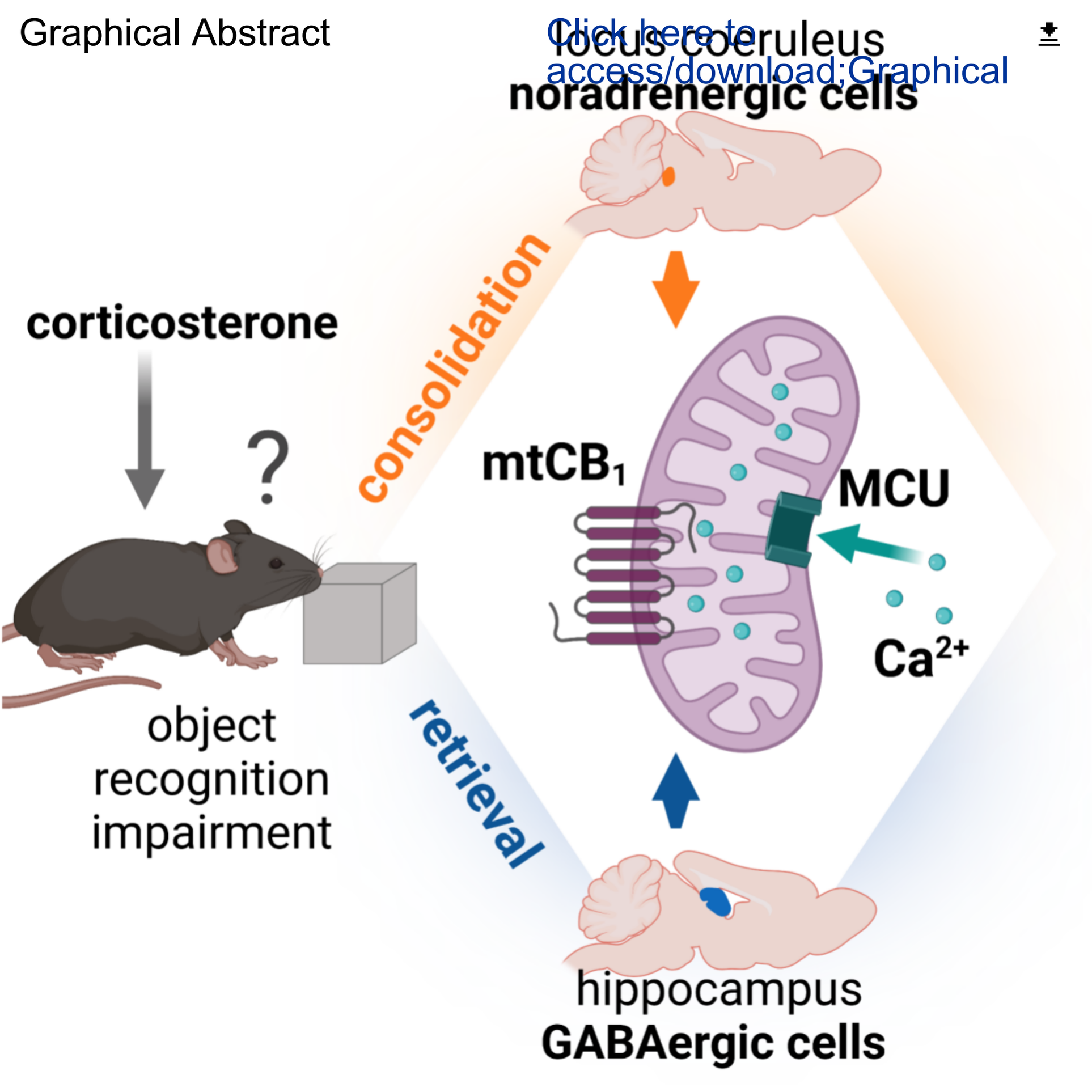

Mitochondrial cannabinoid receptors gate corticosterone impact on novel object recognition

Urszula Skupio[1,2], Julia Welte[1,2], Roman Serrat[1,2], Abel Eraso-Pichot[1,2], Francisca Julio-Kalajzić[1,2], Doriane Gisquet[1,2], Astrid Cannich[1,2], Sebastien Delcasso[3], Isabelle Matias[1,2], Unai B. Fundazuri[1,2], Sandrine Pouvreau[1,2], Antonio C. Pagano Zottola[1,2,4], Gianluca Lavanco[1,2], Inigo Ruiz de Azua[5,6], Beat Lutz[5,6], Luigi Bellocchio[1,2], Arnau Busquets-Garcia[7], Francis Chaouloff[1,2,8], Giovanni Marsicano[1,2,8#]

[1]INSERM, U1215 NeuroCentre Magendie, Bordeaux, 33077, France.
[2]University of Bordeaux, Bordeaux, 33077, France.
[3]Aquineuro, Begles, 33130, France.
[4]Institute for Cellular Biochemistry and Genetics, UMR 5095, Bordeaux, 33077, France.
[5]Institute of Physiological Chemistry, University Medical Center, Mainz, 55131 Germany.
[6]Leibniz Institute for Resilience Research (LIR), Mainz, 55122, Germany.
[7]Cell-type mechanisms in normal and pathological behavior Research Group, Neuroscience Program, IMIM Hospital del Mar Medical Research Institute, Barcelona, 08003, Spain.
[8]These authors share senior authorship
[#]Lead contact: giovanni.marsicano@inserm.fr

SUMMARY

Corticosteroid-mediated stress responses require the activation of complex brain circuits involving mitochondrial activity, but the underlying cellular and molecular mechanisms are scantly known. The endocannabinoid system is implicated in stress coping and it can directly regulate brain mitochondrial functions via type-1 cannabinoid receptors (CB_1) associated with mitochondria membranes ($mtCB_1$). In this study, we show that the impairing effect of corticosterone in the novel object recognition (NOR) task in mice requires $mtCB_1$ receptors and the regulation of mitochondrial calcium levels in neurons. Different brain circuits are modulated by this mechanism to mediate the impact of corticosterone on specific phases of the task. Thus, whereas corticosterone recruits $mtCB_1$ receptors in noradrenergic neurons to impair NOR consolidation, $mtCB_1$ receptors in local hippocampal GABAergic interneurons are required to inhibit NOR retrieval. These data reveal unforeseen mechanisms mediating the effects of corticosteroids during different phases of NOR, involving mitochondrial calcium alterations in different brain circuits.

INTRODUCTION

Through the action of corticosteroid hormones, stress elicits a cascade of energy-demanding biological mechanisms aimed at promoting the survival of the organism[1,2]. However, these protective events come with a cost. For instance, both stress and corticosteroids have been shown to impair different cognitive tasks, such as the consolidation and retrieval of memory[3–8].

A growing body of evidence points to the endocannabinoid system as a major regulator of various physiological and behavioral stress responses[9–11], including alterations in novel object recognition (NOR) task[12]. The endocannabinoid system controls cellular activity in the brain in a highly specific and localized manner, mainly through the activation of type-1 cannabinoid (CB_1) receptors largely localized at presynaptic neuronal plasma membranes[13].

However, functional CB_1 receptors can also be found intracellularly[14]. In particular, a small but functionally significant portion of CB_1 receptors is associated to mitochondrial membranes (termed $mtCB_1$ receptors thereafter) in different brain cells[14–16] and in other organs[17–20], where they modulate several mitochondrial functions, such as oxygen consumption, ATP production, glucose metabolism, ROS generation and regulation of cellular calcium dynamics[14,16,21–23]. Through their effects on synaptic transmission and plasticity on different brain circuits, the aforementioned mitochondrial processes impact specific behavioral functions, such as locomotion and nociception[24], social interactions[22] and memory performance[21]. However, these data have been obtained using the pharmacological administration of exogenous CB_1 receptor agonists. It is well known that, likely due to lack of spatial and temporal specificities, the exogenous activation of CB_1 receptors does not always reflect the physiological functions of the endocannabinoid system[25]. Indeed, no data are available so far concerning the involvement of mitochondrial processes in the endogenous behavioral functions of CB_1 receptors. For instance, it has been suggested that the endocannabinoid control over brain bioenergetics might play a potentially important

physiological role in the effects of stress[9], but until now the involvement of mtCB$_1$ receptors in stress-related circuits has remained unknown.

Several studies have proposed the existence of complex interactions across corticosteroid, noradrenergic, GABAergic and endocannabinoid signaling in several brain regions[26–31]. However, the exact mechanisms mediating these interactions and the potential involvement of mitochondrial processes therein are still largely unknown.

Here, we aimed at elucidating the involvement of CB$_1$ receptors at different cellular and subcellular locations in the acute effects of corticosterone and stress on novel object recognition (NOR) consolidation and retrieval in mice. We found that mtCB$_1$ receptors and the regulation of mitochondrial calcium uptake are required during both phases of memory processing although this relies on two different neuronal circuits. Thus, these data reveal how the same molecular pathway in different circuits can mediate distinct processes within the same cognitive task.

RESULTS

Corticosterone engages mtCB$_1$ receptors in distinct cell populations to impair novel object recognition.

Similar to previously described effects of stress[12,32], we observed that the administration of corticosterone at a dose of 10 mg/kg (subcutaneous, sc), but not 1 or 5 mg/kg, impaired NOR consolidation (injection 30 min after training) or retrieval (injection 30 min before test) in wild-type mice (WT, Figure 1A-D, Figure S1A-B). This effect was not due to unspecific effects of the stress hormone on exploratory behavior, because mice injected with 10 mg/kg corticosterone before the training phase of NOR spent the same time exploring the novel identical objects as vehicle-treated ones (Figure S1C). As expected[33], the injection of 10 mg/kg corticosterone resulted in higher plasma corticosterone levels than foot shock stress (Figure S1D). However, this treatment, besides impacting on NOR performance without altering exploratory behavior *per se*, resulted in an increase of hippocampal 2-AG levels (Figure S1E) comparable to previously demonstrated effects of stress[12,34,35]. Thus, this dose was chosen to investigate the involvement of CB$_1$ receptors in the effects of corticosterone on NOR.

CB$_1$ receptors are present in many different brain cell populations and at various subcellular locations, where they exert very diverse and specific functions[13]. Thus, using different constitutive or conditional *CB$_1$* knock-out (KO) or knock-in (KI) mice (see Methods), we next evaluated which specific subpopulations of CB$_1$ receptors are involved in the corticosterone-induced impairments of NOR consolidation and retrieval. We found that corticosterone injection during consolidation did not influence the NOR performance of global *CB$_1$*-KO mice (Figure 1E, Figure S1F), whereas it impaired this behavior in mice lacking the CB$_1$ receptor either in cortical glutamatergic neurons (Glu-*CB$_1$*-KO, Figure 1F, Figure S1G) or in forebrain GABAergic neurons (GABA-*CB$_1$*-KO, Figure 1G, Figure S1H). Similarly to previous findings using acute stress[12], this effect was abolished in mice lacking *CB$_1$* receptors in noradrenergic cells (DBH-*CB$_1$*-KO, Figure 1H, Figure S1I). In order to study the potential pathophysiological roles of mtCB$_1$ receptors, we recently generated a knock-in mouse line, which expresses the mutant

DN22-CB_1 protein instead of wild-type CB_1 (Ref. 24). DN22-CB_1 lacks the first 22 amino acids of the protein sequence, resulting in a functional receptor that is, however, excluded from mitochondrial membranes[24]. Thus, *DN22-CB_1*-KI mice express functional CB_1 receptors, except the ones associated with mitochondria ("no-mt*CB_1*" mice; see Refs. 21 and 24 for details on the approach and description of the mutant line). Strikingly, corticosterone-induced impairment of NOR consolidation was abolished in DN22-*CB_1*-KI mice (Figure 1I, Figure S1J), suggesting that an endocannabinoid regulation of mitochondrial functions is involved in this effect.

The impairing effect of corticosterone on NOR retrieval was also abolished in global *CB_1*-KO mice (Figure 1J, Figure S2A), and it was not altered in Glu-*CB_1*-KO mice (Figure 1K, Figure S2B). Opposite to consolidation, however, the corticosterone effect during retrieval was completely prevented in GABA-*CB_1*-KO mice (Figure 1L, Figure S2C), whilst it remained unaltered in mice lacking CB_1 receptor expression in noradrenergic neurons (DBH-*CB_1*-KO, Figure 1M, Figure S2D). Finally, as for consolidation, the effect of corticosterone on retrieval was absent in *DN22-CB_1*-KI mice (Figure 1N, Figure S2E).

Altogether, these results demonstrate that corticosterone engages CB_1 receptors in distinct cell types to alter novelty preference at specific stages of the NOR task, namely noradrenergic cells during consolidation and forebrain GABAergic cells during retrieval. Accordingly, it was previously described that CB_1 receptors in noradrenergic cells are key in the impairing effect of foot shock stress on NOR consolidation[12]. However, the impact of stress on NOR retrieval has not been addressed so far. Thus, we observed that foot shock stress exposure 30 min before retrieval impaired NOR in WT, but not in their GABA-*CB_1*-KO littermates (Figure 1O-Q, Figure S2F). Furthermore, we observed that mutant mice, in which CB_1 receptor expression is rescued either globally or specifically in GABAergic cells, displayed corticosterone-induced NOR retrieval impairment (Figure 1P, Figure S2G). These results indicated that “GABAergic” CB_1 receptors are not only necessary, but also sufficient for the impairing effects of corticosterone and stress on NOR retrieval. Finally, by testing specific Cre-expressing mouse lines, we controlled that the mere presence of Cre in noradrenergic or

GABAergic cells is not sufficient to alter the NOR-impairing effects of corticosterone (Figure S2H-K).

As indicated above, one remarkable observation is that corticosterone failed to impair both consolidation (Figure 1I) and retrieval (Figure 1N) of NOR in *DN22-CB$_1$*-KI mice. We therefore hypothesized that mtCB$_1$ receptors in noradrenergic and GABAergic cells might be responsible for the effects of corticosterone during NOR consolidation and retrieval, respectively. We tested this hypothesis by a targeted re-expression approach in mutant mice[24]. Cre-dependent viral vectors were locally injected to re-express either CB$_1$ or DN22-CB$_1$ in DBH-*CB$_1$*-KO or GABA-*CB$_1$*-KO mice (Figure 2A-B). To target noradrenergic neurons, DBH-*CB$_1$*-KO mice (expressing Cre in DBH-positive noradrenergic cells), were injected with viral vectors into the locus coeruleus (LC) to generate LC-DBH-*CB$_1$*-RS and LC-DBH-*DN22-CB$_1$*-RS (RS standing for "rescue", Figure 2C). The hippocampus (HIP) of GABA-*CB$_1$*-KO mice (expressing Cre in Dlx5/6-positive GABAergic cells) was targeted to generate HIP-GABA-*CB$_1$*-RS or HIP-GABA-*DN22-CB$_1$*-RS (Figure 2D). The re-expression of CB$_1$ receptors in the LC of DBH-*CB$_1$*-KO mice (LC-DBH-*CB$_1$*-RS) rescued corticosterone-induced impairment of NOR consolidation, whereas control virus injection (DBH-*CB$_1$*-KO-control) or expression of DN22-CB$_1$ (LC-DBH-*DN22-CB$_1$*-RS) was not able to restore this effect (Figure 2E, Figure S3A). Likewise, whereas CB$_1$ re-expression in the HIP of GABA-*CB$_1$*-KO mice (HIP-GABA-*CB$_1$*-RS) restored the impairing effect of corticosterone on NOR retrieval, no such effect was observed in mice injected with the control virus (GABA-*CB$_1$*-KO-control) and in mice with hippocampal re-expression of DN22-CB$_1$ (HIP-GABA-*DN22-CB$_1$*-RS, Figure 2F, Figure S3B). These results clearly indicate that corticosterone administered during the consolidation phase of NOR alters novelty preference by recruiting mtCB$_1$ receptors in noradrenergic neurons, whereas activation of mtCB$_1$ receptors in local hippocampal GABAergic interneurons is required to impair NOR during retrieval.

Alterations in mitochondrial calcium levels underlies corticosterone-induced impairment of novel object recognition.

As a next step, we aimed at identifying potential molecular mechanisms through which corticosterone-dependent activation of mtCB$_1$ receptors might alter mouse behavior at different stages of the NOR task. It was previously described that exogenous cannabinoids impact memory by acting at mtCB$_1$ receptors to inhibit soluble adenylyl cyclase (sAC)-dependent mitochondrial respiration in the hippocampus[21]. Thus, we first hypothesized that corticosterone might alter NOR performance *via* mtCB$_1$ receptor-dependent regulation of mitochondrial respiration. Oxygen consumption assays revealed that corticosterone injection in WT mice failed to induce changes in mitochondrial respiration in the hippocampus when compared to vehicle injection (Figure S4A), suggesting that mtCB$_1$ receptor-dependent control of mitochondrial respiration is unlikely to be responsible for the NOR effects of the stress hormone. However, this bulk tissue approach did not allow identifying potential effects of corticosterone on specific cell types. To overcome this limitation, we used viral vectors to Cre-dependently overexpress mitochondrial-targeted sAC (mt-sAC)[21,36] in the LC of DBH-Cre mice or in the hippocampus of Dlx-Cre mice, respectively. Importantly, this approach was recently shown to fully block mt*CB$_1$*-dependent effects of exogenous cannabinoids on NOR[21] and on catalepsy[24]. Here, these manipulations however failed to alter corticosterone-induced impairment of NOR consolidation or retrieval, respectively (Figure 3A-B, Figure S4B-C). These data suggest that, in contrast to previously described effects of exogenous cannabinoids[21,24], the NOR-impairing effects caused by corticosterone-induced mobilization of endocannabinoids, likely does not involve mtCB$_1$-dependent inhibition of cellular respiration.

Another recent study showed that, by enhancing mitochondrial calcium uptake, mtCB$_1$ receptors can regulate cytosolic calcium dynamics independently of their impact on sAC signaling and cellular respiration[23]. Therefore, we next addressed the potential role of mitochondrial calcium signaling in the NOR-impairing effects of corticosterone. First, using a fiber photometry approach, we assessed whether mitochondrial calcium movements were modified in mice performing the NOR task upon corticosterone or vehicle administration. To record mitochondrial calcium changes, we used a virus Cre-dependently expressing the calcium sensor GCaMP6s (AAV-DIO-mitoGCaMP6s)[23]

targeted to the mitochondrial matrix. Sensor injection into the hippocampal CA1 area of Dlx-Cre mice (expressing Cre in GABAergic neurons[37]) led to a reliable expression of the sensor (Figure 3C) and hence appropriate fiber photometric recordings of mitochondrial calcium events in GABAergic interneurons of freely-moving behaving animals (Figure 3C). In the L-maze, changes in fluorescence levels were detected when mice were approaching, but not when they were exploring the objects (see Methods; Figure 3D) both during training and testing sessions of the task. During training, no significant difference was noted between the amplitude of calcium signals detected when mice were approaching each of the 2 identical objects presented on either ends of the maze (Figure S4D). Of note, however, the amplitude of calcium signals during the test was decreased when control mice were approaching the novel object, as compared to the familiar one (Figure 3E). Strikingly, this was not the case after a NOR-impairing corticosterone treatment, whereupon no significant differences between the signal amplitudes were observed between the approach towards novel or familiar objects (Figure 3E,F; Figure S4E). Consistently, plotting the difference between novel and familiar transient amplitudes *versus* the discrimination index values revealed a correlation between these two variables (Figure 3G), suggesting that the greater the novelty decreased transient amplitudes, the better mice performed in the NOR task. Based on these results, we hypothesized that mitochondrial calcium dynamics might be involved in the corticosterone-induced impairment of NOR retrieval.

We recently showed that the $mtCB_1$-dependent control of astroglial mitochondrial calcium levels requires the activation of protein kinase B (also known as Akt), leading to the regulation of the mitochondrial calcium uniporter (MCU) channel *via* the Akt-dependent phosphorylation of the MCU modulator, namely mitochondrial calcium uptake protein 1 (MICU1)[23]. Thus, we aimed at testing the involvement of the Akt pathway and of MCU activity in the effects of corticosterone on consolidation or retrieval of NOR in LC noradrenergic or hippocampal GABAergic neurons, respectively. First, we observed that levels of phosphorylated Akt (pAkt) in the hippocampus were increased 30 min after corticosterone injection (Figure S4F), without affecting total Akt expression, indicating that the administration of the stress hormone engages the Akt pathway.

Consistently, pretreatment with the Akt inhibitor MK-2206 (intraperitoneal, i.p., 10 mg/kg) blocked the effects of corticosterone on both NOR consolidation and retrieval (Figure S4G-J). These data suggest that Akt/MCU signaling might underlie the mtCB1-dependent effects of corticosterone on NOR performance. However, although powerful tools, pharmacological treatments intrinsically lack cell type specificity. Moreover, the Akt cascade is involved in many different cellular processes, making it very difficult to single out specific pathways. Therefore, to specifically investigate the role of MCU in identified cell types, we adopted a viral approach to Cre-dependently express a non-phosphorylatable form of the main MCU regulator MICU1 (MICU-S124A)[38] in the LC of DBH-Cre mice or in the dorsal HIP of Dlx-Cre mice, respectively. Strikingly, the expression of MICU-S124A in noradrenergic cells blocked corticosterone-induced NOR impairment of consolidation (Figure 3H, Figure S4K). Similarly, MICU-S124A expression in hippocampal GABAergic cells blocked the retrieval-impairing effect of corticosterone (Figure 3I, Figure S4L). These results link the effects of corticosterone on NOR to the regulation of the Akt/MICU1 signaling pathway in specific neuronal circuits.

DISCUSSION

Our study shows that the stress hormone corticosterone alters exploratory behavior when administered during different phases of the novel object recognition task, doing so through a common molecular mechanism in specific brain circuits. Particularly, we show that mtCB$_1$ receptor activation and regulation of mitochondrial calcium uptake in noradrenergic neurons is responsible for NOR consolidation impairment, while the same mechanism in local hippocampal GABAergic interneurons is necessary to impair NOR retrieval. The dose of corticosterone used here was the minimal one able to impair consolidation and retrieval of the NOR task in our experimental conditions. However, this dose induced higher plasma corticosterone levels than a single foot shock stress, which results in the same behavioral effects[12]. This suggests that additional factors discriminate stress experience from corticosterone injections. Indeed, despite its central role, corticosterone release is not the only effector of the much larger signaling

processes triggered by endogenous stress experience. In this study, we aimed at singling out the mechanisms specifically triggered by the stress hormone to impair identified phases of NOR, and we revealed the capital importance of mitochondrial CB_1 receptors and calcium signaling in these processes. Future studies will address whether and by which ways the additional components of stress responses also involve similar mechanisms. It is of note, however, that exogenous corticosterone and endogenous stress share at least the involvement of "noradrenergic" and "GABAergic" CB_1 receptors in the impairment of NOR consolidation and retrieval, respectively (Ref. 12 and present results). Indeed, the observation that CB_1 receptors in noradrenergic neurons are necessary for corticosterone-induced impairment of novelty recognition is in agreement with a previous study showing that the same subpopulation of CB_1 receptors is both necessary and sufficient for endogenous stress-induced impairment of NOR consolidation[12]. Interestingly, we show here that this particular CB_1 receptor subpopulation is dispensable for corticosterone-induced impairment of NOR retrieval, the latter being accounted for by CB_1 receptors in hippocampal GABAergic interneurons. Moreover, "GABAergic" CB_1 receptors are also necessary and sufficient for foot shock stress-induced impairment of NOR retrieval. Thus, the impact of the stress hormone corticosterone on consolidation or retrieval of NOR is specifically mediated by a CB_1 receptor-dependent control of distinct brain circuits. Whereas noradrenergic neurons in the LC and GABAergic interneurons in the hippocampus are necessary for the impairing effects of corticosterone during different stages of the NOR task, corticosterone exerts widespread effects on the brain[1]. Therefore, it will be interesting in the future to investigate whether other brain structures and pathways are also involved in the behavioral effects observed in this study. In particular, the parallel involvement of other noradrenergic (e.g. in the nucleus of the stria terminalis) or GABAergic neuronal populations (e.g. in other cortical or subcortical brain regions than hippocampus) cannot be excluded at present.

During the last decades, several studies started to address in detail the importance of mitochondrial processes in brain functions[2]. Thus, the regulation of mitochondrial activity emerged as a powerful signaling process to control behavior. For

instance, modulation of mitochondrial respiration and/or dynamics are key determinants of stress responses and social hierarchy[39,40]. Similarly, recent data showed a link between mitochondrial functions and cognition in both animals[41,42] and humans[43]. In this context, the discovery that CB_1 receptors can be associated with mitochondrial membranes in different brain cell types[14,15] suggested the possibility that some of the effects and functions of (endo)cannabinoids might involve mitochondrial alterations. Whereas this idea has been confirmed in several behavioral effects of exogenous cannabinoids[14,16,21–24], no data were so far available concerning the endogenous impact of $mtCB_1$ receptors on behavioral functions. The present results show that corticosterone triggers the endogenous mobilization of endocannabinoids to activate $mtCB_1$ receptors in different circuits to alter NOR consolidation or retrieval.

As mentioned above, we previously showed that $mtCB_1$ receptors are crucial for cannabinoid-induced impairment of NOR[21]. Surprisingly, however, our present results indicate that corticosterone- and cannabinoid-induced NOR impairment are both mediated by mt*CB1* receptors, but *via* different molecular mechanisms. Exogenous cannabinoids impact novelty recognition *via* an $mtCB_1$-dependent decrease of mitochondrial respiration in the hippocampus, involving intra-mitochondrial Gαi protein activation, inhibition of soluble-adenylyl cyclase (sAC), reduced mitochondrial protein kinase A activity and eventual decreased phosphorylation of specific mitochondrial respiratory complex proteins[21]. The present data however show that this pathway is not involved in the corticosterone effects on NOR. $MtCB_1$ receptors were recently reported to modulate calcium dynamics in astrocytes *via* a cascade involving Akt kinase and mitochondrial calcium uniporter (MCU) activities[23]. Strikingly, our data show that these same mechanisms, albeit in neurons, are responsible for the impairment of NOR performance by exogenous corticosterone. Indeed, both the LC "noradrenergic" and hippocampal "GABAergic" $mtCB_1$-dependent corticosterone inhibition of consolidation and retrieval of NOR, respectively, are blocked by pharmacologically or genetically manipulating Akt signaling or MCU activity.

In vivo fiber photometry experiments show a link between mitochondrial calcium dynamics and novelty preference during the NOR task. Specifically, when mice

approach the novel object during test trials, the amplitude of mitochondrial calcium sensor signals in hippocampal GABAergic cells is decreased as compared to the familiar object. Importantly, corticosterone administration before memory retrieval prevents this decrease, suggesting that this effect might be linked to the associated NOR impairment. Considering that activation of $mtCB_1$ receptors increases mitochondrial calcium levels[23], it is tempting to speculate that corticosterone administration impedes this novelty-induced reduction of mitochondrial calcium uptake, thereby disrupting NOR retrieval.

In line with the rising acknowledgement that mitochondrial calcium signaling is important for cognitive processes, recent studies proposed that abnormally high mitochondrial calcium levels lead to memory deficits in mouse models of schizophrenia and Alzheimer's disease[44,45]. Moreover, although the involvement of MCU in cognition is currently poorly investigated, it is interesting to note that disruption of the MCU and MICU1 functions results in memory alterations in drosophila and in a rat model of Alzheimer's disease[46,47].

Overall, our findings unravel unforeseen mechanisms mediating the negative effects of stress and corticosteroids on NOR consolidation and retrieval, involving $mtCB_1$-dependent mitochondrial calcium alterations in different brain circuits. Thus, the modulation of mitochondrial processes and/or $mtCB_1$ receptor signaling might contribute to pave the way to a novel field of research linking mitochondrial calcium uptake to cognitive processes and might represent a promising avenue for the treatment of stress-related cognitive impairments.

Acknowledgments

We would like to thank Delphine Gonzales, Nathalie Aubailly, Elizabeth Huc and all personnel of the Animal Facilities of the NeuroCentre Magendie for mouse care. We thank the Biochemistry Platform, Analytical Chemistry Platform and Genotyping Platform of Bordeaux NeuroCampus for help. We would like to thank dr Geoffrey Terral for his support and help with fiber photometry data analysis. We also thank all members of Marsicano's lab for useful discussions and advice. Graphical abstract was created with BioRender.com. This work was funded by INSERM, the European Research Council (MiCaBra, ERC-2017-AdG-786467 to GM), the Fondation pour la Recherche Medicale (FRM; SPF201809006908 to US, SPF201909009268 to AEP.), Agence Nationale de la Recherche (ANR; NeuroNutriSens ANR-13-BSV4-0006 and ORUPS ANR-16-CE37-0010-01; ERA-Net Neuron CanShank, ANR-21-NEU2-0001-04); University of Bordeaux's IdEx "Investments for the Future" program / GPR BRAIN_2030, and MINECO from AEI (RYC-2017-21776) to ABG.

Author contributions

US, ABG, FC and GM designed the study. US and JW performed viral injections and behavioral experiments. UF and GL assisted in behavioral experiments. US performed and analyzed fiber photometry experiments with assistance of RS and SD. AEP, ACPZ and IM performed biochemical experiments. US performed data analysis. JW, FJK and DG performed immunohistochemistry and image acquisition. AC prepared plasmids and viral vectors. SP generated the mitoGCaMP probe. IRA and BL provided DBH-CB_1 transgenic animals. US and GM wrote the manuscript. IRA, BL, LB and SP provided feedback on the manuscript. ABG, FC and GM supervised the research. All authors edited and approved the manuscript.

Declaration of interests

The authors declare no competing interests.

Inclusion and diversity

One or more of the authors of this paper self-identifies as a member of the LGBTQIA+ community.

Figure titles and legends

Figure 1. Corticosterone acts via different *CB$_1$* receptor populations to impair NOR consolidation or retrieval.

(**A-D**) Dose response experiments show that corticosterone treatment at a dose of 10 mg/kg, but not 1 or 5 mg/kg (sc) during consolidation (30 minutes after training; **A,B**) and before retrieval (30 minutes before final testing; **C,D**) results in NOR impairment in WT mice.

(**E-I**) Impact of corticosterone (10 mg/kg, s.c.) or its vehicle on NOR consolidation in WT mice (**E-I**), in global *CB$_1$*-KO mice (**E**), in Glu-*CB$_1$*-KO mice (**F**), GABA-*CB$_1$*-KO mice (**G**), in DBH-*CB$_1$*-KO (**H**), and in DN22-*CB$_1$*-KI mice (**I**).

(**J-N**) Impact of corticosterone (10 mg/kg, s.c.) or its vehicle on NOR retrieval in WT mice (**J-N**), in global *CB$_1$*-KO mice (**J**), in Glu-*CB$_1$*-KO mice (**K**), in GABA-*CB$_1$*-KO mice (**L**), in DBH-*CB$_1$*-KO (**M**), and in DN22-*CB$_1$*-KI mice (**N**).

(**O-Q**) Impact of stress (single 2 sec 0.5 mA foot-shock) on retrieval of NOR testing session (30 minutes before final testing, **O**) in WT and GABA-*CB$_1$*-KO mice (**Q**). Control animals remained undisturbed in the home cage.

(**P**) Effect of corticosterone injected before NOR retrieval in STOP-*CB$_1$* mice (equivalent to global *CB$_1$*-KO mice), in mice carrying CB_1 receptor re-expression either globally (*CB$_1$*-RS) or specifically in GABAergic cells (GABA-*CB$_1$*-RS).

Please refer to Figures S1 and S2 for exact durations of exploration of novel and familiar objects and total exploration times of each mouse. Significant differences detected in post-hoc analysis are marked with **p<0.01, ***p<0.001; ns- not significant. Significant effect of treatment is marked with ###p<0.001. Data presented as mean ± SEM. Statistical tests and numbers of animals used are described in Table S1.

Figure 2. Corticosterone-induced impairment of NOR is mediated by mtCB$_1$ in distinct cell populations at different memory stages.

(**A,B**) Viral strategy to Cre-dependently re-express *CB$_1$* or DN22-*CB$_1$*, which excludes mitochondrial *CB$_1$* re-expression, in the LC of DBH-*CB$_1$*-KO mice (**A**) or in the dorsal HIP of GABA-*CB$_1$*-KO mice (**B**)

(**C**) Representative immunofluorescent image from DBH-*CB$_1$*-KO mice injected with AAV-DIO-ctr (DBH-*CB$_1$*-KO-control), AAV-DIO-*CB$_1$*-myc (LC-DBH-*CB$_1$*-RS) or AAV-DIO-DN22-*CB$_1$*-myc (LC-DBH-DN22-*CB$_1$*-RS) in the locus coeruleus (LC). TH is in red, c-myc tag in green. Scale bar: 100 μm.

(**D**) Representative immunofluorescent image from GABA-*CB$_1$*-KO mice injected with AAV-DIO-ctr (GABA-*CB$_1$*-KO-control), AAV-DIO-*CB$_1$*-GFP (HIP-GABA-*CB$_1$*-RS) or AAV-DIO-DN22-*CB$_1$*-GFP (HIP-GABA-DN22-*CB$_1$*-RS) into the dorsal HIP. DG- Dentate gyrus. DAPI is in blue, GFP in green. Scale bar: 200 μm.

(**E**) Rescue of CB$_1$ (LC-DBH-*CB$_1$*-RS), but not DN22-CB$_1$ (LC-DBH-DN22-*CB$_1$*-RS) in LC of DBH-*CB$_1$*-KO mice restores the impairing effect of corticosterone on NOR consolidation.

(**F**) Hippocampal rescue of CB$_1$ expression (HIP-GABA-*CB$_1$*-RS), but not DN22-*CB$_1$* (HIP-GABA-DN22-*CB$_1$*-RS) in GABA-*CB$_1$*-KO mice restores the impairing effect of corticosterone on NOR retrieval.

Exact durations of exploration of novel and familiar objects and total exploration times of each mouse are presented in Figure S3. Significant differences detected in post-hoc analysis are marked with ***p<0.001; ns- not significant. Data presented as mean ± SEM. Statistical tests and numbers of animals used are described in Table S1.

Figure 3. Corticosterone impacts memory *via* regulation of mitochondrial calcium.

(**A**) Left panel: Representative immunofluorescent images from WT (control) and DBH-Cre+ littermate mice injected with an AAV virus into LC to Cre-dependently overexpress mt-sAC in DBH-positive cells. Tyrosine hydroxylase (TH) is stained in red, Hemagglutinin (HA) tag in green. Scale bar: 100 μm. Right panel: Both control mice and mice overexpressing mt-sAC in the LC noradrenergic neurons exhibit corticosterone-induced impairment of NOR consolidation.

(**B**) Left panel: Representative immunofluorescent images from WT (control) and Dlx5/6-Cre+ littermate mice injected into the dorsal HIP with an AAV virus to Cre-dependently overexpress mt-sAC in hippocampal interneurons. DAPI is in blue, HA tag in green. Scale bar: 200 μm. DG, Dentate gyrus. Right panel: Both control mice and mice overexpressing mt-sAC in HIP GABAergic cells exhibit corticosterone- induced impairment of NOR retrieval.

(**C**) Left panels: Viral strategy to Cre-dependently express mitoGCaMP6s in hippocampal GABAergic cells of Dlx5/6-Cre+ mice. Below: Representative image of mitoGCaMP6s expression. DAPI is marked in blue, mitoGCaMP6s in green. Scale bar: 200 μm. DG- Dentate gyrus. Right panel: Example of bulk mitoGCaMP6s signal recorded during NOR testing session. ΔF/F represents the fluorescent changes from the mean level of entire recording time series.

(**D**) Example of filtered mitoGCaMP6s signal (the same as presented in **C**) recorded from CA1 GABAergic cells paired with mouse behavior (“approach”, top panel and “exploration”, bottom panel) during NOR test. Colored triangles represent calcium transients detected during approach behavior. No calcium transients were detected during exploration. ΔF/F represents the fluorescent changes from the mean level of entire recording time series.

(**E**) Calcium transient amplitude is significantly decreased during the approach towards the novel object as compared to the familiar object in vehicle-treated, but not in corticosterone-treated, animals.

(**F**) Injection of corticosterone before the retrieval impairs NOR in mice that underwent *in vivo* fiber photometry recordings.

(**G**) Changes in calcium transient amplitude during the test session inversely correlate with NOR discrimination index.

(**H**) Left panel: Representative immunofluorescent image from DBH-Cre mice injected into LC with an AAV virus to Cre-dependently express a non-phosphorylatable form of MICU1 (MICU-S124A). TH is in red, HA tag in green. Scale bar: 100 μm. Right panel: Expression of MICU-S124A in LC of DBH-Cre+ mice prevents corticosterone-induced impairment of NOR consolidation.

(**I**) Left panel: Representative immunofluorescent image from Dlx-Cre mice injected into the HIP with an AAV virus to Cre-dependently express MICU-S124A. DAPI is in blue, HA tag in green. Scale bar: 200 μm. DG- Dentate gyrus. Right panel: Expression of non- phosphorylatable form of MICU in the HIP of Dlx-Cre+ mice blocks corticosterone-induced impairment of NOR retrieval.

For exact times of exploration of novel and familiar objects as well as total exploration times of each mouse please see Figure S4. Significant differences detected in post-hoc analysis are marked with **p<0.01, ***p<0.001; ns- not significant. Significant effect of treatment is marked with ###p<0.001. Data presented as mean ± SEM. All statistical tests and numbers of animals used are described in Table S1.

STAR Methods

RESOURCE AVAILABILITY

Lead contact

Further information and requests for resources and reagents should be directed to and will be fulfilled by the lead contact, Giovanni Marsicano (giovanni.marsicano@inserm.fr).

Materials availability

Viral vectors, plasmids and mouse lines are available on request.

Data and code availability

- All data obtained in this study is available from the lead contact upon request.
- Original code used to analyze fiber photometry has been deposited at Zenodo and is publicly available as of the date of publication. DOI is listed in the key resources table.
- Any additional information required to reanalyze the data reported in this paper is available from the lead contact upon request.

EXPERIMENTAL MODEL AND SUBJECT DETAILS

Animals

This study involved 2-4 months old male C57BL/6N mice purchased from Janvier (France) as well as male 2-4 months old constitutive and conditional CB_1 receptor mutant and WT mice, established in breeding facilities of Neurocentre Magendie (Bordeaux, France) since 2006. These mice included: CB_1-floxed mice, constitutive line of full CB_1 receptor knockout (*CB_1*-KO) mice[49], conditional knockout mice lacking CB_1 receptors in cortical glutamatergic neurons due to expression of Nex-Cre recombinase (Glu-*CB_1*-KO)[37], conditional knockout mice lacking CB_1 in forebrain GABAergic neurons due to Dlx5/6-Cre expression (GABA-*CB_1*-KO)[37], conditional knockout mice lacking CB_1 in noradrenergic neurons due to DBH-Cre expression (DBH-*CB_1*-KO)[12,50], mice

expressing Cre recombinase in Dlx5/6 positive cells (Dlx-Cre) or DBH-positive cells (DBH-Cre), knock-in mice which lack mitochondria-associated CB_1 (DN22-*CB_1*-KI) that were generated using a flox-stop strategy to replace wild type CB_1 receptor by the mutant version of CB_1 protein lacking the first 22 amino acids (called DN22-CB_1), which results in almost full reduction of CB_1 mitochondrial targeting[21,24], with the functionality of the DN22-CB_1 protein as a cannabinoid receptor maintained as presented by P-ERK and G proteins increases upon cannabinoid stimulation comparable to wild-type CB_1 receptor[21,24]. Wild-type littermates of each mouse line were used as control groups. Furthermore, to evaluate whether CB_1 receptors on GABAergic neurons are sufficient for corticosterone-induced impairment of NOR, we used a rescue approach, whereby CB_1 receptor function is suppressed globally in STOP-*CB_1* mice by a transcriptional Stop cassette flanked by two loxP sites and inserted into the 5′ UTR of the ORF-containing CB_1 receptor exon[51]. Mice bearing selective rescue of CB_1 receptor expression in GABAergic neurons (GABA-*CB_1*-RS) were generated by crossing STOP-CB_1 mice with Dlx-Cre mice, whereas WT equivalent controls were generated by crossing STOP-*CB_1* mice with the general Cre-deleter mouse line EIIa-Cre (*CB_1*-RS)[51]. All mutant and WT mice, bred in a mixed genetic background with a predominant C57BL/6N contribution, were genotyped at 2–3 weeks old and regenotyped at the end of experiments. Due to well characterized sex differences in reactivity of the corticotropic axis[48], we have used only male mice in the present study. Potential sex differences in the crosstalk of corticosteroid and endocannabinoid systems in our experimental approach will be addressed in future studies.

All animal procedures were conducted in accordance with standard ethical guidelines (European Directive 2010/63/UE). Experiments were approved by the local ethical committee and the French Ministry of Agriculture and Forestry (authorization number APAFIS#22372-2019101017185578). Mice were housed collectively under standard conditions with food and water ad libitum, 12 h light–dark cycle with lights on at 7:00 am, in temperature- and humidity-controlled room. All experiments were performed during the light phase. Animals were handled daily for 3-5 days before the start of experiments.

METHOD DETAILS

Drug preparation and administration

Corticosterone (Sigma-Aldrich, C22505), at doses ranging from 1-10 mg/kg, was first mixed for 20-30 min in 80% ethanol (VWR Chemicals, 20821), 20% saline (Virbac, 0055) solution at 37°C, 1000 rpm, until dissolved. Next, warm (37°C) saline was added to reach a final concentration of vehicle at 5% of ethanol. Corticosterone solution was freshly prepared for every experiment and administered subcutaneously (s.c.) 30 min after training session of NOR task (described below) to study its influence on consolidation, or 30 min before testing session to study its effects on retrieval. Akt – inhibitor MK-2206 (Enzo Life Sciences, ENZ-CHM164) was dissolved in a mixture of 7% DMSO (Sigma-Aldrich, D5879), 1.25% Tween-80 (Sigma-Aldrich, P1754) and saline. It was prepared freshly before experiments at a dose of 10 mg/kg and injected intraperitoneally (i.p.) 10 min before corticosterone treatment. Corresponding vehicle solutions were used in control experiments. All treatments were administered at a volume of 10 ml/kg.

Plasmids

Plasmids for Cre-dependent rescue of CB_1 and DN22-CB_1 were achieved as previously described[24]. The plasmid encoding for MICU1-S124A [38] was a generous gift from Prof. Paolo Pinton (University of Ferrara, Italy). The plasmid coding for Mito-GCaMP6s was obtained using standard cloning techniques a previously described [23].

Viral vectors

To generate AAV-DIO-*CB_1*-Myc, AAV-DIO-DN22-*CB_1*-Myc, AAV-DIO-mt-sAC-HA, AAV-DIO-MICU-S124A-HA and AAV-DIO-mito-GCaMP6s the coding sequences for the 5 proteins were sub-cloned into AAV-CAG-DIO plasmid (kindly gifted by Matthias Klugmann, UNSW, Australia) by using standard molecular cloning techniques [24]. The same pAAV-CAG-DIO plasmid was used as empty control (AAV-DIO-ctr) [24]. AAVs were generated by PEI transfection of HEK293T cells and purified by iodixanol-gradient

ultracentrifugation as previously described[21,24]. Virus titers were: $1.76*10^{10}$ for AAV-DIO-ctrl, $7*10^{10}$-$3.3*10^{11}$ for AAV-DIO-CB_1-Myc, $3.4*10^{10}$-$7.4*10^{11}$ for AAV-DIO-DN22-CB_1-Myc, $8.3*10^{10}$ for AAV-DIO-CB_1-GFP, $8.7*10^{10}$ for AAV-DIO-DN22-CB_1-GFP, $7.4*10^{10}$ for AAV-DIO-mt-sAC-HA, $4.6*10^{10}$ for AAV-DIO-mito-GCaMP6s and $4.7*10^{10}$ for AAV-DIO-MICU-S124A-HA, expressed as genomic copies (GC) per ml.

Surgery and viral vectors administration

Mice were anesthetized using 5% isoflurane and placed into the stereotaxic apparatus (David Kopf Instruments) with mouse adaptor and lateral ear bars, and the isoflurane was maintained at 1.5-2% during the entire surgery. Subcutaneous buprenorphine (0.05 mg/kg, Buprecare) and lidocaine (0.1 ml at 0.5%, Lidor) at the level of the skull were injected prior to surgery to induce analgesia. A heating-pad was positioned underneath the animal to keep the body temperature at 37°C. Eye dehydration was prevented by topical application of ophthalmic gel. The skin above the skull was shaved with an electric razor and disinfected with iodine solution (Betadine) before an incision was made. Viral vectors were injected with the help of a glass pipette attached to a microinjector (Nanoject III, Drummond Scientific) or a microsyringe (10µl Hamilton syringe with a 30-gauge bevelled needle) attached to a pump (UMP3-1, World Precision Instruments). To target the dorsal hippocampus, mice were injected bilaterally with 1000 nl per injection site (in case of CB_1/DN22-CB_1 re-expression and mt-sAC experiments), or 500 nl per injection site (in case of MICU-S124A experiment) at a rate of 250 nl per minute, with the following coordinates (from Bregma): AP -1.8, ML ± 1.0, DV -2.0 and -1.5. To target locus coeruleus, mice were injected bilaterally with 150 nl per injection site at a rate of 120 nl per minute (for all experiments), with the following coordinates (from Bregma): AP -5.3, ML ±0.85, DV -3.75. For fiber photometry experiments, mice were injected unilaterally into the dorsal hippocampus with 400 nl of virus at a rate of 60 nl per minute, with the following coordinates (from Bregma): AP -2.2, ML -2.0, DV -1.5. The optical fiber (400 µm diameter) was placed 200 µm above the injection site and fixed with dental cement (MajorRepair). Following any virus delivery, the syringe/pipette was left in place for at least 4 min before being slowly withdrawn from the brain. Following surgery, all mice received ip injection of 0.2 ml of

saline solution and anti-inflammatory drug meloxicam (5 mg/kg, Metacam), that was continued for additional 2 days. Animals continued to be housed collectively and body weight was monitored daily during 4-5 days to assess recovery. Behavioral experiments were carried out 4-5 weeks after surgery and fiber photometry experiments 5-6 weeks after surgery.

Viral expression

For all intra-LC viral injections, tagged viruses were found to be expressed in the entire LC. For intra-HIP injections, with the exception of fiber photometry experiment, tagged viruses were found to be spread in the anterior part of dorsal hippocampus (-1.3 to -2.2 from Bregma), with fluorescent signals detected in CA1, CA3 and dentate gyrus (DG). In the posterior part of dorsal hippocampus (from -2.2 to -2.8 from Bregma), fluorescent signals were detected sporadically, mostly in CA1 area. For the fiber photometry experiment, fluorescent signal of mitoGCamp6s was found largely in CA1 and sparsely in CA2 and CA3 areas of the anterior part of dorsal hippocampus (-1.3 to -2.2 from Bregma), fibers were placed above CA1.

Novel object recognition test

The task was performed in a L-shaped maze with dark grey walls (35 cm and 30 cm long respectively for external and internal L walls, 4.5 cm wide and 15 cm high walls) placed on a light grey tabletop, in a room adjacent to the animal house with a light intensity fixed at 30 lux measured at the top of the maze. The maze was overhung by a video camera allowing the detection and offline scoring of animal's behavior. The task consisted of 3 sequential daily trials of 9 minutes each. On the first day, during the habituation phase, mouse was placed in the center of the maze and allowed to freely explore the arms in the absence of any objects. The following day, during the training phase, mouse was placed again in the center of the maze in the presence of two identical objects positioned at the extremities of each arm and left to freely explore the maze and the objects. The testing phase occurred on the third day: one of the familiar objects was replaced by a novel object different in its shape, color and texture and mice

were left to explore both objects. The position of the novel object and the associations of novel and familiar were randomized. All objects were previously tested to avoid biased preference. Memory performance was assessed in two ways: either by direct comparison of exploration times between familiar and novel objects within each group (presented in supplementary figures), or by using the discrimination index (DI) to compare between groups (presented in main text). The DI was calculated as the difference between the time spent exploring the novel (TN) and the familiar object (TF) divided by the total exploration time (TN+TF): DI = [TN-TF]/[TN+TF]. Object exploration was defined as direct contact of the nose with the object. Climbing on top of the object was not considered as exploration. Experienced investigators evaluating the exploration were blinded to genotype of the animals.

Fiber photometry recordings and data analysis

Freely-moving mice were imaged using 470 and 405 nm LEDs to excite Mito-GCaMP6s 5-6 weeks after surgery, after 5 days of handling and habituation to attach the fiber. To record the fluorescence signals, the fiber photometry system was custom-made and configured as previously described [23]. The wavelength for Mito-GCaMP6 excitation was 470 nm (blue light), while the isosbestic wavelength is 405 nm (UV light). The isosbestic stimulation was used in alternation with the blue light to treat the signal after, as the fluorescence emitted after this stimulation is not depending on calcium [52]. The Mito-GCaMP6s fluorescence from hippocampal interneurons was collected with a sCMOS camera (Hamamatsu Orca Flash v3) through an optic fiber (core 400 µm, N.A 0.49) divided in 2 sections: a short fiber implanted in the brain of the mouse and a long fiber (modified patchcord), both connected through a ferrule-ferrule (1.25 mm) connection. To minimize the photobleaching effect of the recording and preserve a high signal to noise ratio, the light intensities in the tip of the patch cord were adjusted to ~130 µW for the 470 nm channel and ~80 µW for the 405 nm channel. A custom MATLAB script (Matlabworks) was used to synchronize video recording with fiber photometry, combined with a programmed Arduino board. The sampling rate was settled at 20 Hz for both photometry and video recording.

Novel object recognition was performed like described above and video recorded. Behavior of animals was later scored manually with object “exploration” defined as any period of time in which the test mouse was actively investigating the object. Investigation included direct contact of the nose with the object. Climbing on top of the object was not considered as exploration. “Approach” was defined as period of time in which mouse was passing from one L-maze arm to the other, moving towards the object until the nose was approximately 2 cm away from the object.

Obtained fiber photometry signal was analyzed using custom MATLAB scripts. The first minute of the recording was removed to decrease the effect of primary exponential decrease due to photo bleaching on the linear fit made after in the analysis pipeline. The isobestic signal was fitted (linear fitting) to the 470 nm signal. Then, for each time point, ΔF/F was calculated as (F470nm - F405nm(fitted))/F405nm(fitted); Lerner et al., 2015). In order to detect the transients, the ΔF/F signal was filtered using a bandpass butterworth filter of order 4 (0,02 Hz, 0,14Hz, empirically determined on few randomly chosen traces). Finally, peaks having a prominence superior to 0.1 (empirically chosen) of the bandpass filtered signal were collected as transients. Calcium transients detected during “approach” behavior were rescaled using min-max normalization. For almost all recordings, only one calcium transient was detected for each “approach” behavior, therefore frequency of events was not analyzed. Likewise, almost no calcium transients were detected when mice were exploring the objects, therefore no analysis of calcium signal was performed for this behavior. Mean normalized amplitudes of ΔF/F were calculated across all calcium transients associated with either behavior, and the difference was analyzed using a 2-way ANOVA.

Measurement of endocannabinoid levels

Mice underwent 5 days of handling and 3 days of habituation to sc injections. On the day of the experiment, mice were injected with vehicle or corticosterone (10 mg/kg, sc) and sacrificed 30 min later by dislocation. Hippocampal tissues were isolated, weighted and quickly frozen in dry ice. To detect hippocampal levels of anandamide (AEA) and 2-arachidonoylglycerol (2-AG), the tissue was homogenized, lipids were

extracted, and samples were analyzed by liquid chromatography-tandem mass spectrometry (LC-MS/MS) in the Analytical Chemistry platform of the Neurocentre Magendie like described before[53]. In brief, samples were homogenized and extracted with chloroform/methanol/Tris-HCl 50 mM pH 7.5 (2:1:1, v/v) containing internal deuterated standards (AEA-d4 and 2-AG-d5). The dried lipid extract was pre-purified by open bed chromatography on silica columns eluted with increasing concentrations of methanol in chloroform if necessary. Fractions for AEA and 2-AG measurement were obtained by eluting the column with 9:1 (by vol.) chloroform/methanol and were concentrated on an N2 stream evaporator. Samples were then subjected to liquid chromatography-chemical ionization-tandem mass spectrometric analysis (LC-MSMS). Mass spectral analyses were performed on a TSQ Quantum triple quadrupole instrument (Thermo-Finnigan) equipped with an atmospheric pressure chemical ionisation (APCI) source and operating in positive ion mode. A sensitive and specific LC-MSMS method was developed and validated for endocannabinoid quantification. The concentrations of AEA and 2-AG were determined using a calibration curve and normalized to the tissue weight. Final results of two independent experiments were normalized to the mean of the control groups of respective experiments and pooled together.

Measurement of plasma corticosterone levels

For quantification of corticosterone levels in blood plasma, mice were treated with vehicle, corticosterone (10 mg/kg) or received a vehicle injection and a single 0.5 mA footshock. Animals were sacrificed 30 min later by decapitation, trunk blood samples were collected in K3 Ethylenediaminetetraacetic acid (EDTA) micro sample tubes (Sarstedt). Blood plasma was obtained by a centrifugation step at 10000 x g for 10 min using a microcentrifuge (VWR). The resulting layer of blood plasma was collected. Corticosterone levels were measured by performing enzyme-linked immunosorbent assay (ELISA) analysis following the manufacturer's instructions (DetectX Corticosterone Immunoassay Kit; Arbor Assays). In brief, samples were mixed 1:1 with Dissociation Reagent and incubated at room temperature (RT) for 5 min. All samples were then diluted in Assay Buffer at a ratio of 1:1000. Samples were pipetted

into the wells. Then DetectX® Corticosterone Conjugate (25µl) and DetectX® Corticosterone Antibody (25µl) were added and the plate was incubated at RT for 1 h while shaking at 700-900 rpm. Wells were washed 4 times with 300 µL of wash buffer, 100 µL of the TMB Substrate was added to each well and plate was incubated at RT for 30 min without shaking. After adding 50 µL of Stop Solution to each well, the optical density (OD) generated in each well was immediately read using the POLARstar Omega plate reader (BMG Labtech).

Hippocampal respiration

Mitochondrial hippocampal respiration was measured as previously described[24]. Briefly, mice injected with corticosterone (10 mg/kg) or vehicle were sacrificed 10 or 30 minutes after injection, brain was extracted and both hippocampi were immediately dissected and homogenized in 450 µL of Miro5 buffer without taurine supplementation using a Politron homogenizer (11,000 rpm 3-5 s). After brief centrifugation, saponin (12.5 µg/ml) was added to the supernatant. 30 µl of the sample was diluted in 2 ml Mir05 buffer and respiration analysis were carried out using a 2K Oroboros device. Basal respiration corresponds to the oxygen consumption of enriched mitochondria in the presence of malate (2 mM), pyruvate (5 mM) and glutamate (10 mM) (MPG). Complex I dependent respiration was measured by adding ADP (5 mM) to the chambers.

Western blot

Mice were sacrificed 30 minutes after corticosterone (10 mg/kg) or vehicle injection, hippocampi were dissected and stored at -80°C until analysis. Hippocampi were processed as previously described[54]. Mixed with denaturing 4x Laemmli loading buffer, protein extracts were heated for 5 min at 95°C. Samples (50 µg per lane) were separated on 4%–20% precast polyacrylamide gels (Bio-Rad, Hercules, California) and transferred onto PVDF membranes 0.45 µm (Merk Millipore, Billerica, MA). Membranes were soaked in TBS-T (20 mM Tris-HCl pH 7.6, 150mM NaCl, 0.05% Tween 20) containing 5% of bovine serum albumin for 1 h at room temperature (RT) and incubated

with antibodies against phospho-Akt (Ser473) (#9271, 1:1000, overnight 4°C, Cell Signaling Technology Danvers, MA). After stripping and re-blocking with TBS-T 5% non-fat dry milk, membranes were probed with antibodies against Akt (pan) (#2920, 1:1000, overnight 4°C, Cell Signaling Technology Danvers, MA) and Tubulin (sc-69969; 1:5000, 1h RT Santa Cruz Biotechnology, Dallas, Texas). Primary antibodies were detected with HRP-linked secondary antibodies (1:2000, 1 h RT Cell Signaling Technology, Danvers, MA) by enhanced chemiluminescence (Clarity Western ECL Substrate, Bio-Rad, Hercules, California or Super Signal West Femto Maximum Sensitivity Substrate, Thermo Fisher Scientific, Waltham, MA). Labeling was analyzed using Image Lab software (Bio-Rad, Hercules, California) after the acquisition on ChemiDoc Touch (Bio-Rad, Hercules, California).

Perfusion

Mice were deeply anesthetized by intraperitoneal injection of pentobarbital (Exagon, Axience SAS, 400 mg/kg body weight). Mice were transcardially perfused with phosphate-buffered solution (PBS 0.1M, pH 7.4) before being fixed with 4% formaldehyde (Sigma, HT501128-4L). Brains were isolated and post fixated in the same fixative solution overnight at 4ºC, then transferred to a 30% (wt/vol) sucrose (Sigma, S0389) solution for cryopreservation and finally frozen in isopentane (Sigma-Aldrich, M32631) and stored at -80°C. Free-floating frozen coronal sections (40 µm) were cut out using a cryostat (Leica Biosystems, CM1950S). The cryosections were collected in antifreeze solution and conserved at -20°C until further use.

Fluorescence immunohistochemistry on free-floating sections.

Immuno-detection in the hippocampus:

Immuno-detection of C-myc epitope tag – The endogenous peroxidases were inactivated by incubating the free-floating sections with 3% H2O2 in PBS-DEPC for 30 minutes. Sections were permeabilized in a blocking solution (in PBS: 10% donkey serum, 0.3% Triton X-100) for 1 hour at room temperature (RT). Then, sections were incubated with a rabbit primary antibody against the C-myc epitope tag (1:500, Cell

Signaling #2278) overnight at 4°C. After several washes with PBS, slices were incubated for 2 hours with a secondary antibody goat anti rabbit HRP linked antibody (1:500, Cell Signalling #7074) and then washed in PBS at RT. The signal of C-myc tag was revealed by a TSA reaction using fluorescein isothiocyanate (FITC)-labeled tyramide (1:250 for 10 minutes, Perkin Elmer). Finally, sections were incubated with 4',6-diamidino-2-phenylindole (DAPI 1:20000, Invitrogen D3571) diluted in PBS to visualize cell nuclei and then were washed, mounted and coverslipped. The sections were imaged with fluorescence microscope (Leica Microsystems CMS GmBbH, Type: 11504197; SerNo.: 389934).

Immuno-detection of HA epitope tag – Sections were permeabilized in a blocking solution (in PBS: 10% donkey serum, 0.3% Triton X-100) for 1 hour at room temperature (RT). Then, sections were incubated with a rabbit primary antibody against the HA epitope tag (1:500, Cell Signaling #3724) overnight at 4°C. After several washes with PBS, slices were incubated for 2 hours with a secondary antibody donkey anti rabbit alexa fluor 488 (1:500, Invitrogen A21206) and then washed in PBS at RT. Finally, sections were incubated with 4',6-diamidino-2-phenylindole (DAPI 1:20000, Invitrogen D3571) diluted in PBS to visualize cell nuclei and then were washed, mounted and coverslipped. The sections were imaged with fluorescence microscope (Leica Microsystems CMS GmBbH, Type: 11504197; SerNo.: 389934).

Immuno-detection of GFP – Sections were permeabilized in a blocking solution (in PBS: 10% donkey serum, 0.3% Triton X-100) for 1 hour at room temperature (RT). Then, sections were incubated with a rabbit primary antibody against GFP (1:1000, Invitrogen, #A11122) overnight at 4°C. After several washes with PBS, slices were incubated for 2 hours with a secondary antibody donkey anti rabbit alexa fluor 488 (1:500, Invitrogen A21206) and then washed in PBS at RT. Finally, sections were incubated with 4',6-diamidino-2-phenylindole (DAPI 1:20000, Invitrogen D3571) diluted in PBS to visualize cell nuclei and then were washed, mounted and coverslipped. The sections were imaged with fluorescence microscope (Leica Microsystems CMS GmBbH, Type: 11504197; SerNo.: 389934).

Immuno-detection in locus coeruleus (LC):

Coimmuno-detection of C-myc epitope tag and tyrosine hydroxylase (TH) – The endogenous peroxidases were inactivated by incubating the free-floating sections with 3% H2O2 in PBS-DEPC for 30 minutes. Sections were permeabilized in a blocking solution (in PBS: 10% donkey serum, 0.3% Triton X-100) for 1 hour at room temperature (RT). Then, sections were incubated with a mix of primary antibodies: rabbit antibody against the C-myc epitope tag (1:500, Cell Signaling #2278) and mouse antibody monoclonal against TH (1:5000 Milipore, MAB318) overnight at 4°C. After several washes with PBS, slices were incubated for 2 hours at RT with a mix of secondary antibodies: goat anti rabbit HRP linked antibody (1:500, Cell Signalling #7074) and donkey anti mouse alexa fluor 555 (1:500, Invitrogen A31570). Then, sections were washed in PBS at RT. The signal of C-myc tag was revealed by a TSA reaction using fluorescein isothiocyanate (FITC)-labeled tyramide (1:250 for 10 minutes, Perkin Elmer). Finally, sections were incubated with 4',6-diamidino-2-phenylindole (DAPI 1:20000, Invitrogen D3571) diluted in PBS to visualize cell nuclei and then were washed, mounted and coverslipped. The sections were imaged with fluorescence microscope (Leica Microsystems CMS GmBbH, Type: 11504197; SerNo.: 389934).

Coimmuno-detection of HA epitope tag and tyrosine hydroxylase (TH) – Sections were permeabilized in a blocking solution (in PBS: 10% donkey serum, 0.3% Triton X-100) for 1 hour at room temperature (RT). Then, sections were incubated with a mix of primary antibodies: rabbit antibody against the HA epitope tag (1:500, Cell Signaling #3724) and mouse antibody monoclonal against TH (1:5000 Milipore, MAB318) overnight at 4°C. After several washes with PBS, slices were incubated for 2 hours at RT with a mix of secondary antibodies: donkey anti rabbit alexa fluor 488 (1:500, Invitrogen A21206) and donkey anti mouse alexa fluor 555 (1:500, Invitrogen A31570). Then sections were washed in PBS at RT. Finally, they were incubated with 4',6-diamidino-2-phenylindole (DAPI 1:20000, Invitrogen D3571) diluted in PBS to visualize cell nuclei and then were washed, mounted and coverslipped. The sections were imaged with fluorescence microscope (Leica Microsystems CMS GmBbH, Type: 11504197; SerNo.: 389934).

QUANTIFICATION AND STATISTICAL ANALYSIS

Data collection

No statistical methods were used to pre-determine sample sizes, but they are similar to those reported in previous publications. All mice were assigned pseudo-randomly to experimental groups. Experimenters were blinded to mice genotypes, but not treatments.

Statistical analyses

Statistical analyses were performed using GraphPad software (version 8.0). Results were expressed as means of independent data ± SEM. All data were checked for normality distribution with the Shapiro-Wilk test. When comparing more than 2 groups, one-way or two-way (where appropriate) analyses of variances (ANOVAs) were performed. When interactions proved significant, Sidak's post hoc analyses were performed. In case when the normality was rejected, non-parametric One-way ANOVA (Kruskal-Wallis) was used. Biochemical and behavioral comparisons between 2 experimental groups were analyzed using Student's t-test (unpaired or paired, where appropriate) or Wilcoxon's test (nonparametric data). Post hoc significances are expressed as follow: * $p < 0.05$, ** $p < 0.01$, *** $p < 0.001$. Sample sizes, used tests and p values of each analysis can be found in Table S1.

Supplemental information titles and legends

Table S1. Statistical analysis details, related to Figures 1-3 and Figures S1-S4.

References

1. McEwen, B.S. (2007). Physiology and neurobiology of stress and adaptation: central role of the brain. Physiol Rev *87*, 873–904. 10.1152/physrev.00041.2006.

2. Picard, M., McEwen, B.S., Epel, E.S., and Sandi, C. (2018). An energetic view of stress: Focus on mitochondria. Frontiers in Neuroendocrinology *49*, 72–85. 10.1016/j.yfrne.2018.01.001.

3. Atsak, P., Roozendaal, B., and Campolongo, P. (2012). Role of the endocannabinoid system in regulating glucocorticoid effects on memory for emotional experiences. Neuroscience *204*, 104–116. 10.1016/j.neuroscience.2011.08.047.

4. de Quervain, D., Schwabe, L., and Roozendaal, B. (2017). Stress, glucocorticoids and memory: implications for treating fear-related disorders. Nat Rev Neurosci *18*, 7–19. 10.1038/nrn.2016.155.

5. Roozendaal, B. (2003). Systems mediating acute glucocorticoid effects on memory consolidation and retrieval. Prog Neuropsychopharmacol Biol Psychiatry *27*, 1213–1223. 10.1016/j.pnpbp.2003.09.015.

6. Roozendaal, B., Okuda, S., de Quervain, D.J.-F., and McGaugh, J.L. (2006). Glucocorticoids interact with emotion-induced noradrenergic activation in influencing different memory functions. Neuroscience *138*, 901–910. 10.1016/j.neuroscience.2005.07.049.

7. Conrad, C.D. (2005). THE RELATIONSHIP BETWEEN ACUTE GLUCOCORTICOID LEVELS AND HIPPOCAMPAL FUNCTION DEPENDS UPON TASK AVERSIVENESS AND MEMORY PROCESSING STAGE. Nonlinearity Biol Toxicol Med *3*, 57–78. 10.1080/15401420490900245.

8. Schwabe, L., Hermans, E.J., Joëls, M., and Roozendaal, B. (2022). Mechanisms of memory under stress. Neuron *110*, 1450–1467. 10.1016/j.neuron.2022.02.020.

9. Lutz, B., Marsicano, G., Maldonado, R., and Hillard, C.J. (2015). The endocannabinoid system in guarding against fear, anxiety and stress. Nat Rev Neurosci *16*, 705–718. 10.1038/nrn4036.

10. Morena, M., Patel, S., Bains, J.S., and Hill, M.N. (2016). Neurobiological Interactions Between Stress and the Endocannabinoid System. Neuropsychopharmacology *41*, 80–102. 10.1038/npp.2015.166.

11. Micale, V., and Drago, F. (2018). Endocannabinoid system, stress and HPA axis. European Journal of Pharmacology *834*, 230–239. 10.1016/j.ejphar.2018.07.039.

12. Busquets-Garcia, A., Gomis-González, M., Srivastava, R.K., Cutando, L., Ortega-Alvaro, A., Ruehle, S., Remmers, F., Bindila, L., Bellocchio, L., Marsicano, G., et

al. (2016). Peripheral and central CB1 cannabinoid receptors control stress-induced impairment of memory consolidation. PNAS *113*, 9904–9909. 10.1073/pnas.1525066113.

13. Busquets-Garcia, A., Bains, J., and Marsicano, G. (2018). CB1 Receptor Signaling in the Brain: Extracting Specificity from Ubiquity. Neuropsychopharmacol. *43*, 4–20. 10.1038/npp.2017.206.

14. Bénard, G., Massa, F., Puente, N., Lourenço, J., Bellocchio, L., Soria-Gómez, E., Matias, I., Delamarre, A., Metna-Laurent, M., Cannich, A., et al. (2012). Mitochondrial CB_1 receptors regulate neuronal energy metabolism. Nat Neurosci *15*, 558–564. 10.1038/nn.3053.

15. Gutiérrez-Rodríguez, A., Bonilla-Del Río, I., Puente, N., Gómez-Urquijo, S.M., Fontaine, C.J., Egaña-Huguet, J., Elezgarai, I., Ruehle, S., Lutz, B., Robin, L.M., et al. (2018). Localization of the cannabinoid type-1 receptor in subcellular astrocyte compartments of mutant mouse hippocampus. Glia *66*, 1417–1431. 10.1002/glia.23314.

16. Koch, M., Varela, L., Kim, J.G., Kim, J.D., Hernández-Nuño, F., Simonds, S.E., Castorena, C.M., Vianna, C.R., Elmquist, J.K., Morozov, Y.M., et al. (2015). Hypothalamic POMC neurons promote cannabinoid-induced feeding. Nature *519*, 45–50. 10.1038/nature14260.

17. Kamnate, A., Sirisin, J., Watanabe, M., Kondo, H., Hipkaeo, W., and Chomphoo, S. (2022). Mitochondrial Localization of CB1 in Progesterone-producing Cells of Ovarian Interstitial Glands of Adult Mice. J Histochem Cytochem *70*, 251–257. 10.1369/00221554211063516.

18. Mendizabal-Zubiaga, J., Melser, S., Bénard, G., Ramos, A., Reguero, L., Arrabal, S., Elezgarai, I., Gerrikagoitia, I., Suarez, J., Rodríguez De Fonseca, F., et al. (2016). Cannabinoid CB1 Receptors Are Localized in Striated Muscle Mitochondria and Regulate Mitochondrial Respiration. Frontiers in Physiology *7*.

19. Rossato, M., Ion Popa, F., Ferigo, M., Clari, G., and Foresta, C. (2005). Human sperm express cannabinoid receptor Cb1, the activation of which inhibits motility, acrosome reaction, and mitochondrial function. J Clin Endocrinol Metab *90*, 984–991. 10.1210/jc.2004-1287.

20. Pagano Zottola, A.C., Severi, I., Cannich, A., Ciofi, P., Cota, D., Marsicano, G., Giordano, A., and Bellocchio, L. (2022). Expression of Functional Cannabinoid Type-1 (CB1) Receptor in Mitochondria of White Adipocytes. Cells *11*, 2582. 10.3390/cells11162582.

21. Hebert-Chatelain, E., Desprez, T., Serrat, R., Bellocchio, L., Soria-Gomez, E., Busquets-Garcia, A., Pagano Zottola, A.C., Delamarre, A., Cannich, A., Vincent, P., et al. (2016). A cannabinoid link between mitochondria and memory. Nature *539*, 555–559. 10.1038/nature20127.

22. Jimenez-Blasco, D., Busquets-Garcia, A., Hebert-Chatelain, E., Serrat, R., Vicente-Gutierrez, C., Ioannidou, C., Gómez-Sotres, P., Lopez-Fabuel, I., Resch-Beusher, M., Resel, E., et al. (2020). Glucose metabolism links astroglial mitochondria to cannabinoid effects. Nature *583*, 603–608. 10.1038/s41586-020-2470-y.

23. Serrat, R., Covelo, A., Kouskoff, V., Delcasso, S., Ruiz-Calvo, A., Chenouard, N., Stella, C., Blancard, C., Salin, B., Julio-Kalajzić, F., et al. (2021). Astroglial ER-mitochondria calcium transfer mediates endocannabinoid-dependent synaptic integration. Cell Rep *37*, 110133. 10.1016/j.celrep.2021.110133.

24. Soria-Gomez, E., Pagano Zottola, A.C., Mariani, Y., Desprez, T., Barresi, M., Bonilla-Del Río, I., Muguruza, C., Le Bon-Jego, M., Julio-Kalajzić, F., Flynn, R., et al. (2021). Subcellular specificity of cannabinoid effects in striatonigral circuits. Neuron *109*, 1513-1526.e11. 10.1016/j.neuron.2021.03.007.

25. Busquets-Garcia, A., Desprez, T., Metna-Laurent, M., Bellocchio, L., Marsicano, G., and Soria-Gomez, E. (2015). Dissecting the cannabinergic control of behavior: The where matters. Bioessays *37*, 1215–1225. 10.1002/bies.201500046.

26. Atsak, P., Hauer, D., Campolongo, P., Schelling, G., Fornari, R.V., and Roozendaal, B. (2015). Endocannabinoid signaling within the basolateral amygdala integrates multiple stress hormone effects on memory consolidation. Neuropsychopharmacology *40*, 1485–1494. 10.1038/npp.2014.334.

27. Barsegyan, A., Mirone, G., Ronzoni, G., Guo, C., Song, Q., van Kuppeveld, D., Schut, E.H.S., Atsak, P., Teurlings, S., McGaugh, J.L., et al. (2019). Glucocorticoid enhancement of recognition memory via basolateral amygdala-driven facilitation of prelimbic cortex interactions. Proc Natl Acad Sci U S A *116*, 7077–7082. 10.1073/pnas.1901513116.

28. Berger, A.L., Henricks, A.M., Lugo, J.M., Wright, H.R., Warrick, C.R., Sticht, M.A., Morena, M., Bonilla, I., Laredo, S.A., Craft, R.M., et al. (2018). The Lateral Habenula Directs Coping Styles Under Conditions of Stress via Recruitment of the Endocannabinoid System. Biol Psychiatry *84*, 611–623. 10.1016/j.biopsych.2018.04.018.

29. Morena, M., Roozendaal, B., Trezza, V., Ratano, P., Peloso, A., Hauer, D., Atsak, P., Trabace, L., Cuomo, V., McGaugh, J.L., et al. (2014). Endogenous cannabinoid release within prefrontal-limbic pathways affects memory consolidation of emotional training. Proc Natl Acad Sci U S A *111*, 18333–18338. 10.1073/pnas.1420285111.

30. Morena, M., Aukema, R.J., Leitl, K.D., Rashid, A.J., Vecchiarelli, H.A., Josselyn, S.A., and Hill, M.N. (2019). Upregulation of Anandamide Hydrolysis in the Basolateral Complex of Amygdala Reduces Fear Memory Expression and Indices of Stress and Anxiety. J Neurosci *39*, 1275–1292. 10.1523/JNEUROSCI.2251-18.2018.

31. Santori, A., Morena, M., Hill, M.N., and Campolongo, P. (2020). Hippocampal 2-Arachidonoyl Glycerol Signaling Regulates Time-of-Day- and Stress-Dependent Effects on Rat Short-Term Memory. Int J Mol Sci *21*, E7316. 10.3390/ijms21197316.

32. Wang, M., Hill, M.N., Zhang, L., Gorzalka, B.B., Hillard, C.J., and Alger, B.E. (2012). Acute Restraint Stress Enhances Hippocampal Endocannabinoid Function via Glucocorticoid Receptor Activation. J Psychopharmacol *26*, 56–70. 10.1177/0269881111409606.

33. de Quervain, D.J., Roozendaal, B., and McGaugh, J.L. (1998). Stress and glucocorticoids impair retrieval of long-term spatial memory. Nature *394*, 787–790. 10.1038/29542.

34. Wang, M., Hill, M.N., Zhang, L., Gorzalka, B.B., Hillard, C.J., and Alger, B.E. (2012). Acute restraint stress enhances hippocampal endocannabinoid function via glucocorticoid receptor activation. J Psychopharmacol *26*, 56–70. 10.1177/0269881111409606.

35. Hill, M.N., McLaughlin, R.J., Pan, B., Fitzgerald, M.L., Roberts, C.J., Lee, T.T.-Y., Karatsoreos, I.N., Mackie, K., Viau, V., Pickel, V.M., et al. (2011). Recruitment of prefrontal cortical endocannabinoid signaling by glucocorticoids contributes to termination of the stress response. J Neurosci *31*, 10506–10515. 10.1523/JNEUROSCI.0496-11.2011.

36. Acin-Perez, R., Salazar, E., Brosel, S., Yang, H., Schon, E.A., and Manfredi, G. (2009). Modulation of mitochondrial protein phosphorylation by soluble adenylyl cyclase ameliorates cytochrome oxidase defects. EMBO Mol Med *1*, 392–406. 10.1002/emmm.200900046.

37. Monory, K., Massa, F., Egertová, M., Eder, M., Blaudzun, H., Westenbroek, R., Kelsch, W., Jacob, W., Marsch, R., Ekker, M., et al. (2006). The Endocannabinoid System Controls Key Epileptogenic Circuits in the Hippocampus. Neuron *51*, 455–466. 10.1016/j.neuron.2006.07.006.

38. Marchi, S., Corricelli, M., Branchini, A., Vitto, V.A.M., Missiroli, S., Morciano, G., Perrone, M., Ferrarese, M., Giorgi, C., Pinotti, M., et al. (2019). Akt-mediated phosphorylation of MICU1 regulates mitochondrial Ca2+ levels and tumor growth. EMBO J *38*, e99435. 10.15252/embj.201899435.

39. Gebara, E., Zanoletti, O., Ghosal, S., Grosse, J., Schneider, B.L., Knott, G., Astori, S., and Sandi, C. (2021). Mitofusin-2 in the Nucleus Accumbens Regulates Anxiety and Depression-like Behaviors Through Mitochondrial and Neuronal Actions. Biol Psychiatry *89*, 1033–1044. 10.1016/j.biopsych.2020.12.003.

40. Hollis, F., van der Kooij, M.A., Zanoletti, O., Lozano, L., Cantó, C., and Sandi, C. (2015). Mitochondrial function in the brain links anxiety with social subordination. Proc Natl Acad Sci U S A *112*, 15486–15491. 10.1073/pnas.1512653112.

41. Hara, Y., Yuk, F., Puri, R., Janssen, W.G.M., Rapp, P.R., and Morrison, J.H. (2014). Presynaptic mitochondrial morphology in monkey prefrontal cortex correlates with working memory and is improved with estrogen treatment. Proc Natl Acad Sci U S A *111*, 486–491. 10.1073/pnas.1311310110.

42. Jacobs, R.A., Aboouf, M.A., Koester-Hegmann, C., Muttathukunnel, P., Laouafa, S., Arias-Reyes, C., Thiersch, M., Soliz, J., Gassmann, M., and Schneider Gasser, E.M. (2021). Erythropoietin promotes hippocampal mitochondrial function and enhances cognition in mice. Commun Biol *4*, 938. 10.1038/s42003-021-02465-8.

43. Apaijai, N., Sriwichaiin, S., Phrommintikul, A., Jaiwongkam, T., Kerdphoo, S., Chansirikarnjana, S., Thongmung, N., Mahantassanapong, U., Vathesatogkit, P., Kitiyakara, C., et al. (2020). Cognitive impairment is associated with mitochondrial dysfunction in peripheral blood mononuclear cells of elderly population. Sci Rep *10*, 21400. 10.1038/s41598-020-78551-4.

44. Devaraju, P., Yu, J., Eddins, D., Mellado-Lagarde, M.M., Earls, L.R., Westmoreland, J.J., Quarato, G., Green, D.R., and Zakharenko, S.S. (2017). Haploinsufficiency of the 22q11.2 microdeletion gene Mrpl40 disrupts short-term synaptic plasticity and working memory through dysregulation of mitochondrial calcium. Mol Psychiatry *22*, 1313–1326. 10.1038/mp.2016.75.

45. Jadiya, P., Kolmetzky, D.W., Tomar, D., Di Meco, A., Lombardi, A.A., Lambert, J.P., Luongo, T.S., Ludtmann, M.H., Praticò, D., and Elrod, J.W. (2019). Impaired mitochondrial calcium efflux contributes to disease progression in models of Alzheimer's disease. Nat Commun *10*, 3885. 10.1038/s41467-019-11813-6.

46. Drago, I., and Davis, R.L. (2016). Inhibiting the Mitochondrial Calcium Uniporter during Development Impairs Memory in Adult Drosophila. Cell Reports *16*, 2763–2776. 10.1016/j.celrep.2016.08.017.

47. Nikseresht, Z., Ahangar, N., Badrikoohi, M., and Babaei, P. (2021). Synergistic enhancing-memory effect of D-serine and RU360, a mitochondrial calcium uniporter blocker in rat model of Alzheimer's disease. Behavioural Brain Research *409*, 113307. 10.1016/j.bbr.2021.113307.

48. Oyola, M.G., and Handa, R.J. (2017). Hypothalamic–pituitary–adrenal and hypothalamic–pituitary–gonadal axes: sex differences in regulation of stress responsivity. Stress *20*, 476–494. 10.1080/10253890.2017.1369523.

49. Marsicano, G., Wotjak, C.T., Azad, S.C., Bisogno, T., Rammes, G., Cascio, M.G., Hermann, H., Tang, J., Hofmann, C., Zieglgänsberger, W., et al. (2002). The endogenous cannabinoid system controls extinction of aversive memories. Nature *418*, 530–534. 10.1038/nature00839.

50. Srivastava, R.K., Ruiz de Azua, I., Conrad, A., Purrio, M., and Lutz, B. (2022). Cannabinoid CB1 Receptor Deletion from Catecholaminergic Neurons Protects from Diet-Induced Obesity. Int J Mol Sci *23*, 12635. 10.3390/ijms232012635.

51. Remmers, F., Lange, M.D., Hamann, M., Ruehle, S., Pape, H.-C., and Lutz, B. (2017). Addressing sufficiency of the CB1 receptor for endocannabinoid-mediated functions through conditional genetic rescue in forebrain GABAergic neurons. Brain Struct Funct *222*, 3431–3452. 10.1007/s00429-017-1411-5.

52. Lütcke, H., Murayama, M., Hahn, T., Margolis, D.J., Astori, S., Zum Alten Borgloh, S.M., Göbel, W., Yang, Y., Tang, W., Kügler, S., et al. (2010). Optical recording of neuronal activity with a genetically-encoded calcium indicator in anesthetized and freely moving mice. Front Neural Circuits *4*, 9. 10.3389/fncir.2010.00009.

53. Dubreucq, S., Matias, I., Cardinal, P., Häring, M., Lutz, B., Marsicano, G., and Chaouloff, F. (2012). Genetic dissection of the role of cannabinoid type-1 receptors in the emotional consequences of repeated social stress in mice. Neuropsychopharmacology *37*, 1885–1900. 10.1038/npp.2012.36.

54. Busquets-Garcia, A., Oliveira da Cruz, J.F., Terral, G., Pagano Zottola, A.C., Soria-Gómez, E., Contini, A., Martin, H., Redon, B., Varilh, M., Ioannidou, C., et al. (2018). Hippocampal CB1 Receptors Control Incidental Associations. Neuron *99*, 1247-1259.e7. 10.1016/j.neuron.2018.08.014.

Key resources table

REAGENT or RESOURCE	SOURCE	IDENTIFIER
Antibodies		
Rabbit anti-cmyc	Cell Signaling Technology	Cat: #2278S; RRID:AB_490778
Mouse anti-Tyrosine Hydroxylase (TH)	Merck Millipore	Cat: MAB318; RRID:AB_2201528
Rabbit anti-HA	Cell Signaling Technology	Cat: #3724S; RRID:AB_1549585
Rabbit anti-GFP	Invitrogen	Cat: #A11122; RRID:AB_221569
Anti-rabbit HRP	Cell Signaling Technology	Cat: #7074S; RRID:AB_2099233
Donkey anti-mouse Alexa 555	Thermo Fisher Scientific	Cat: #A31570; RRID:AB_2536180
Donkey anti rabbit Alexa 488	Thermo Fisher Scientific	Cat: #A21206; RRID:AB_2535792
Tubulin	SantaCruz Biotechnology	Cat: #sc-69969; RRID: AB_1118882
Akt (pan) (40D4) Mouse	Cell Signaling Technology	Cat: #2920; RRID:AB_1147620
Phospho-Akt (Ser473)	Cell Signaling Technology	Cat: #9271; RRID:AB_329825
Bacterial and virus strains		
AAV-DIO-CB1-Myc	This paper	virus n21 lab stock
AAV-DIO-DN22-CB1-Myc	This paper	virus n22 lab stock
AAV-DIO-CB1-GFP	This paper	virus n95 lab stock
AAV-DIO-DN22-CB1-GFP	This paper	virus n96 lab stock
AAV-CAG-DIO-control	This paper	virus n30 lab stock
AAV-DIO-mt-sAC-HA	This paper	virus n5 lab stock
AAV-DIO-mito-GCaMP6s	This paper	virus n76 lab stock
AAV-DIO-MICU-S124A-HA	This paper	virus n98 lab stock
Chemicals, peptides, and recombinant proteins		
Corticosterone	Sigma	Cat: #C22505
MK-2206	Enzo Life Sciences	Cat: # ENZ-CHM164
Experimental models: Organisms/strains		
C57BL/6N mice (WT)	Janvier (France)	N/A
CB1-flox mice (WT)	Neurocenter Magendie (France)	MGI:3045419
full CB1 KO mice, Cnr1tm1.1Ltz, CB1null	Neurocenter Magendie (France)	MGI:2182924
Nex-CB1-KO (Glu-CB1-KO mice)	Monory et al., 2006	N/A
Dlx-CB1-KO (GABA-CB1-KO) mice	Monory et al., 2006	N/A
DBH-CB1-KO mice	prof. Beat Lutz, IMB, Mainz, Germany, Busquets-Garcia et al., 2016	N/A

DN22-CB1-KI mice	Neurocenter Magendie (France), Hebert-Chatelain et al., 2016	N/A
STOP-CB1 mice	Neurocenter Magendie (France), Remmers et al., 2017	N/A
CB1-RS	Neurocenter Magendie (France)	N/A
GABA-CB1-RS	Neurocenter Magendie (France)	N/A
DBH-Cre mice	Neurocenter Magendie (France)	N/A
Dlx-Cre mice	Neurocenter Magendie (France)	N/A
Recombinant DNA		
Mito-GCaMP6s	This paper	N/A
MICU1-S124A	Marchi et al., 2019	N/A
DN22-CB1	Hebet-Chatelain et al., 2016	N/A
Software and algorithms		
GraphPad Prism 8.0	GraphPad	RRID:SCR_002798
ImageJ	ImageJ	RRID:SCR_002285
MATLAB R2018	MATLAB	RRID:SCR_001622
Calcium event analysis code	This paper	DOI: 10.5281/zenodo.7781821

Figure 1

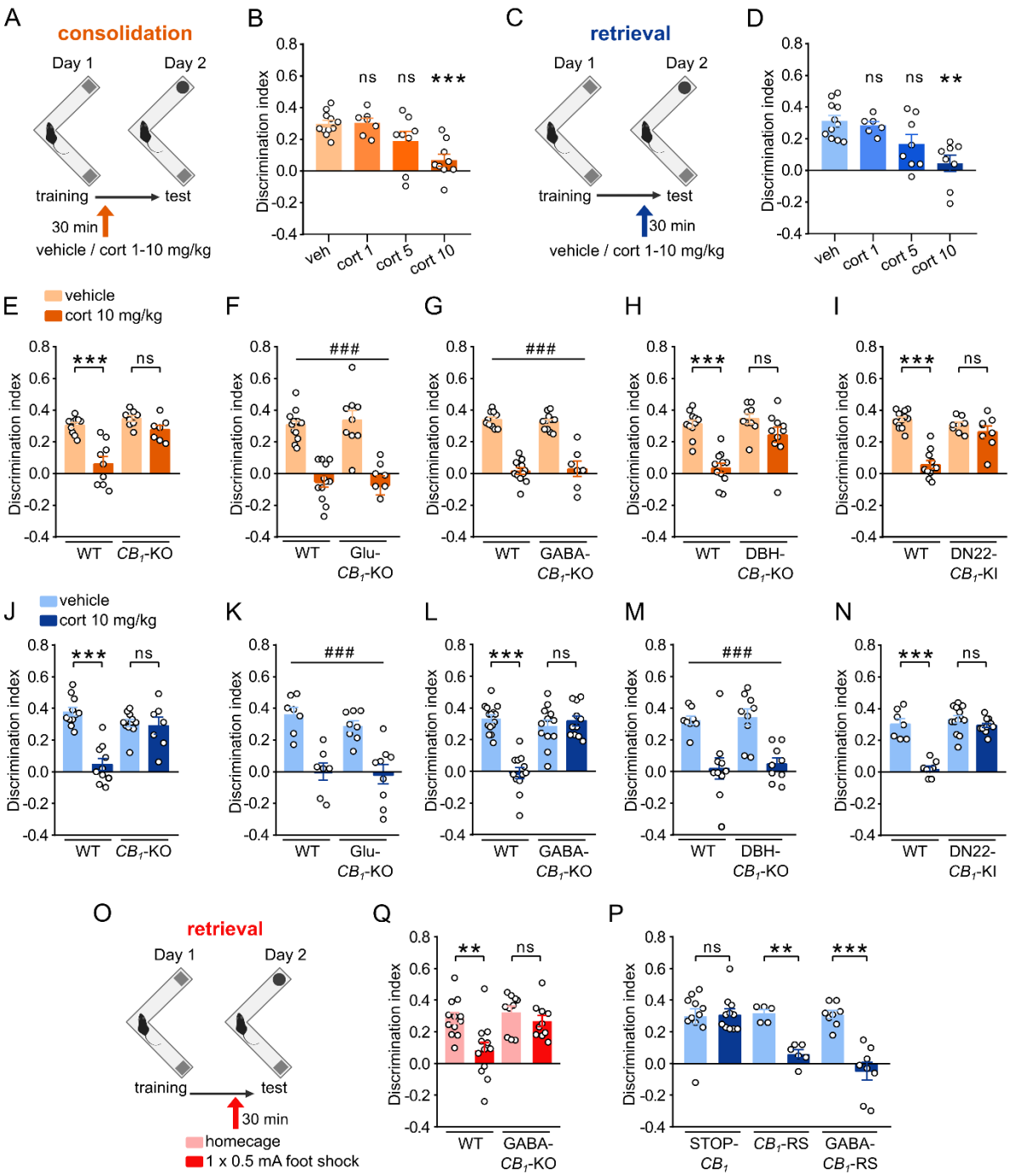
A
consolidation
Day 1
Day 2
training
test
30 min
vehicle / cort 1-10 mg/kg
B
Discrimination index
ns
ns
***
veh
cort 1
cort 5
cort 10
C
retrieval
Day 1
Day 2
training
test
30 min
vehicle / cort 1-10 mg/kg
D
Discrimination index
ns
ns
**
veh
cort 1
cort 5
cort 10
E
vehicle
cort 10 mg/kg
Discrimination index
***
ns
WT
CB1-KO
F
###
WT
Glu-CB1-KO
G
###
WT
GABA-CB1-KO
H
***
ns
WT
DBH-CB1-KO
I
***
ns
WT
DN22-CB1-KI
J
vehicle
cort 10 mg/kg
***
ns
WT
CB1-KO
K
###
WT
Glu-CB1-KO
L
***
ns
WT
GABA-CB1-KO
M
###
WT
DBH-CB1-KO
N
***
ns
WT
DN22-CB1-KI
O
retrieval
Day 1
Day 2
training
test
30 min
homecage
1 x 0.5 mA foot shock
Q
**
ns
WT
GABA-CB1-KO
P
ns
**
***
STOP-CB1
CB1-RS
GABA-CB1-RS

Figure 2

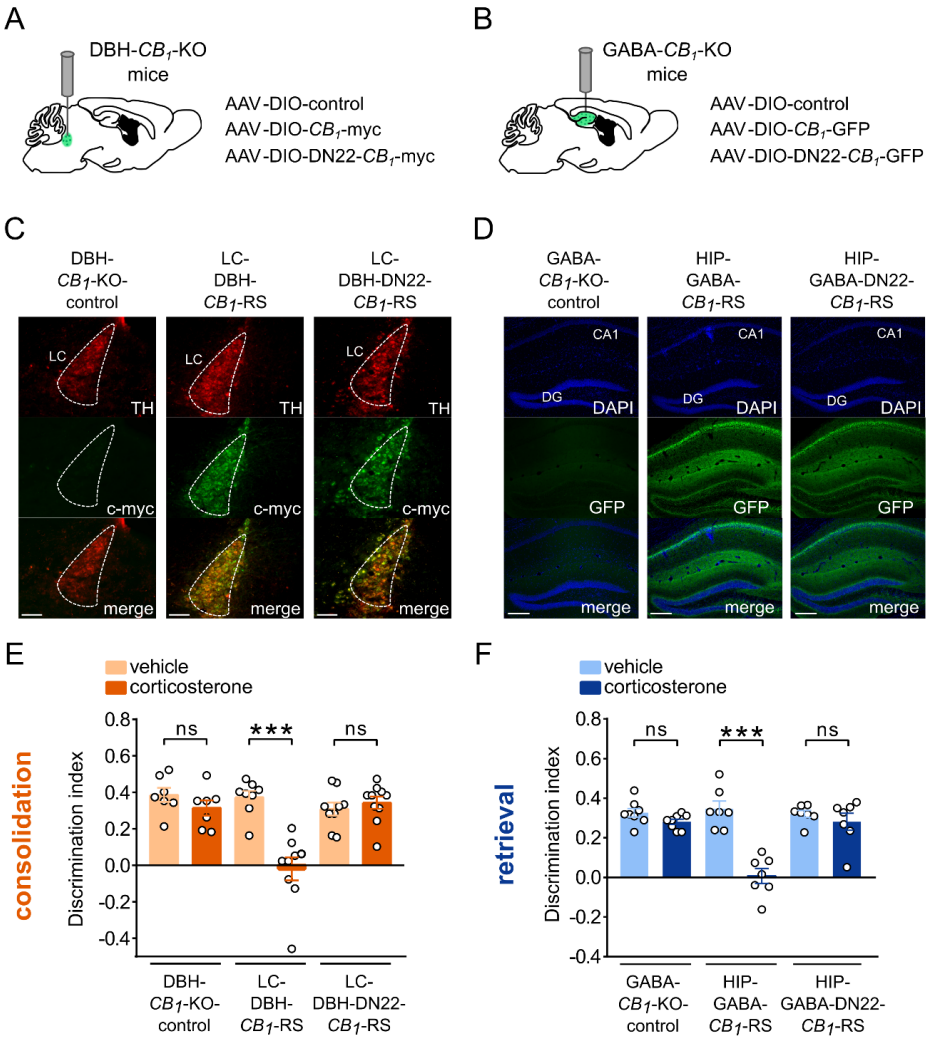
A
DBH-CB1-KO mice
AAV-DIO-control
AAV-DIO-CB1-myc
AAV-DIO-DN22-CB1-myc
B
GABA-CB1-KO mice
AAV-DIO-control
AAV-DIO-CB1-GFP
AAV-DIO-DN22-CB1-GFP
C
DBH-CB1-KO-control
LC-DBH-CB1-RS
LC-DBH-DN22-CB1-RS
LC
TH
c-myc
merge
D
GABA-CB1-KO-control
HIP-GABA-CB1-RS
HIP-GABA-DN22-CB1-RS
CA1
DG
DAPI
GFP
merge
E
vehicle
corticosterone
consolidation
Discrimination index
ns
***
ns
DBH-CB1-KO-control
LC-DBH-CB1-RS
LC-DBH-DN22-CB1-RS
F
vehicle
corticosterone
retrieval
Discrimination index
ns
***
ns
GABA-CB1-KO-control
HIP-GABA-CB1-RS
HIP-GABA-DN22-CB1-RS

Figure 3

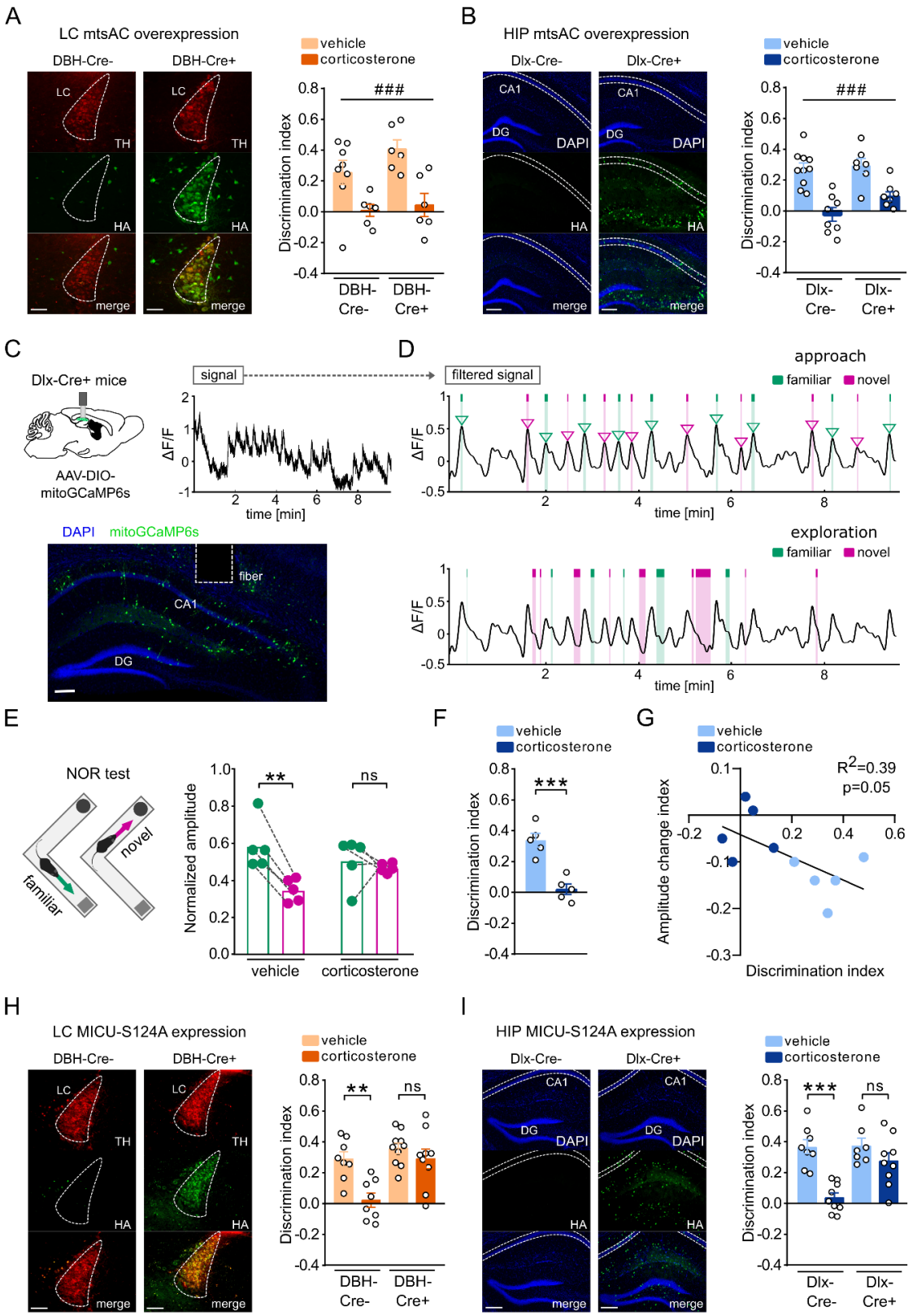
A
LC mtsAC overexpression
DBH-Cre-
DBH-Cre+
LC
TH
HA
merge
vehicle
corticosterone
###
Discrimination index
DBH-Cre-
DBH-Cre+
B
HIP mtsAC overexpression
Dlx-Cre-
Dlx-Cre+
CA1
DG
DAPI
HA
merge
vehicle
corticosterone
###
Discrimination index
Dlx-Cre-
Dlx-Cre+
C
Dlx-Cre+ mice
AAV-DIO-mitoGCaMP6s
signal
ΔF/F
time [min]
DAPI
mitoGCaMP6s
fiber
CA1
DG
D
filtered signal
approach
familiar
novel
ΔF/F
time [min]
exploration
familiar
novel
ΔF/F
time [min]
E
NOR test
familiar
novel
Normalized amplitude
**
ns
vehicle
corticosterone
F
vehicle
corticosterone
***
Discrimination index
G
vehicle
corticosterone
R2=0.39
p=0.05
Amplitude change index
Discrimination index
H
LC MICU-S124A expression
DBH-Cre-
DBH-Cre+
LC
TH
HA
merge
vehicle
corticosterone
**
ns
Discrimination index
DBH-Cre-
DBH-Cre+
I
HIP MICU-S124A expression
Dlx-Cre-
Dlx-Cre+
CA1
DG
DAPI
HA
merge
vehicle
corticosterone
***
ns
Discrimination index
Dlx-Cre-
Dlx-Cre+

Fig.	Figure experiment	Groups	Number of animals per group
MAIN FIGURES:			
1B	Dose-dependent effects of cort injection during NOR consolidation		n=7-11
1D	Dose-dependent effects of cort injection before NOR retrieval		n=6-11
1E	Cort effects on NOR consolidation in full CB1-KO mice		n=7-10
1F	Cort effects on NOR consolidation in Glu-CB1-KO mice		n=8-14
1G	Cort effects on NOR consolidation in GABA-CB1-KO mice		n=10-14
1H	Cort effects on NOR consolidation in DBH-CB1-KO mice		n=9-11
1I	Cort effects on NOR consolidation in DN22-CB1-KI mice		n=8-13
1J	Cort effects on NOR retrieval in full CB1-KO mice		n=7-11
1K	Cort effects on NOR retrieval in Glu-CB1-KO mice		n=7-10
1L	Cort effects on NOR retrieval in GABA-CB1-KO mice		n=11-15
1M	Cort effects on NOR retrieval in DBH-CB1-KO mice		n=8-10
1N	Cort effects on NOR retrieval in DN22-CB1-KI mice		n=7-13
1Q	Foot shock (1x0.5mA) stress effect on NOR retrieval in GABA-CB1-KO mice		n=10-12
1P	Cort effects on NOR retrieval in CB1-RS and GABA-CB1-RS mice		n=5-11
2E	Cort effects on NOR consolidation in LC-CB1-RS and LC-DN22-CB1-RS mice		n=7-10
2F	Cort effects on NOR retrieval in HIP-CB1-RS and HIP-DN22-CB1-RS mice		n=7-8
3A	Cort effects on NOR consolidation in DBH-mtsAC-overexpression experiment		n=6-8
3B	Cort effects on NOR retrieval in GABA-mtsAC-overexpression experiment		n=7-10

3E	Calcium transients amplitude during NOR test in vehicle and cort treated mice		n=5
3F	Cort effect on NOR retieval in in vivo fiber photometry experiment		n=5
3G	Correlation between changes in transients ampliude and NOR discrimination index		n=10
3H	Cort effects on NOR consolidation in LC-MICU-S124A mice		n=8-10
3I	Cort effects on NOR retrieval in HIP-MICU-S124A mice		n=8-9
SUPPLEMENTARY FIGURES			
S1A	Exploration familiar vs novel cort consolidation	veh cort 1 cort 5 cort 10	n=11 n=7 n=8 n=9
	Total exploration times cort consolidation		n=7-11
S1B	Exploration familiar vs novel cort retrieval	veh cort 1 cort 5 cort 10	n=11 n=6 n=8 n=8
	Total exploration times cort rerieval		n=6-11
S1C	Exploration of novel objects during training sesion of NOR after veh or cort administration		n=7
S1D	Plasma corticosterone measured 30 min after foot shock or corticosterone injection	vehicle foot shock cort 10	n=7
S1E	2-AG levels measured 30 min after cort intection		n=11-12
	AEA levels measured 30 min after cort intection		n=11-12
S1F	Exploration familiar vs novel in WT mice	vehicle cort	n=10 n=9
	Exploration familiar vs novel in full CB1-KO mice	vehicle cort	n=8 n=7
	Total exploration times in WT and full CB1-KO mice		n=7-10
S1G	Exploration familiar vs novel in WT mice	vehicle cort	n=14 n=12
	Exploration familiar vs novel in Glu-CB1-KO mice	vehicle cort	n=9 n=8
	Total exploration times in WT and Glu-CB1-KO mice		n=8-14
S1H	Exploration familiar vs novel in WT mice	vehicle cort	n=10 n=13
	Exploration familiar vs novel in GABA-CB1-KO mice	vehicle cort	n=14 n=10

	Total exploration times in WT and GABA-CB1-KO mice		n=10-14
S1I	Exploration familiar vs novel in WT mice	vehicle cort	n=11 n=11
	Exploration familiar vs novel in DBH-CB1-KO mice	vehicle cort	n=9 n=10
	Total exploration times in WT and DBH-CB1-KO mice		n=9-11
S1J	Exploration familiar vs novel in WT mice	vehicle cort	n=13 n=11
	Exploration familiar vs novel in DN22-CB1-KI mice	vehicle cort	n=8 n=8
	Total exploration times in WT and DN22-CB1-KI mice		n=8-13
S2A	Exploration familiar vs novel in WT mice	vehicle cort	n=11 n=10
	Exploration familiar vs novel in full CB1-KO mice	vehicle cort	n=11 n=7
	Total exploration times in WT and full CB1-KO mice		n=7-11
S2B	Exploration familiar vs novel in WT mice	vehicle cort	n=7 n=7
	Exploration familiar vs novel in Glu-CB1-KO mice	vehicle cort	n=8 n=9
	Total exploration times in WT and Glu-CB1-KO mice		n=7-9
S2C	Exploration familiar vs novel in WT mice	vehicle cort	n=15 n=14
	Exploration familiar vs novel in GABA-CB1-KO mice	vehicle cort	n=13 n=11
	Total exploration times in WT and GABA-CB1-KO mice		n=11-15
S2D	Exploration familiar vs novel in WT mice	vehicle cort	n=8 n=10
	Exploration familiar vs novel in DBH-CB1-KO mice	vehicle cort	n=9 n=9
	Total exploration times in WT and DBH-CB1-KO mice		n=8-10
S2E	Exploration familiar vs novel in WT mice	vehicle cort	n=7 n=8
	Exploration familiar vs novel in DN22-CB1-KI mice	vehicle cort	n=13 n=12
	Total exploration times in WT and DN22-CB1-KI mice		n=7-13
	Exploration familiar vs novel in WT mice	vehicle shock	n=12 n=12

S1F	Exploration familiar vs novel in GABA-CB1-KO mice	vehicle shock	n=10 n=10
	Total exploration times in WT and GABA-CB1-KO mice		n=10-12
S2G	Exploration familiar vs novel in STOP-CB1 mice	vehicle cort	n=11 n=11
	Exploration familiar vs novel in CB1-RS mice	vehicle cort	n=5 n=6
	Exploration familiar vs novel in GABA-CB1-RS mice	vehicle cort	n=8 n=8
	Total exploration times in WT, CB1-RS and GABA-CB1-RS mice		n=8-11
S2H	Cort effects on NOR consolidation in DBH-Cre mice		n=6-9
S2I	Exploration familiar vs novel in WT mice	vehicle cort	n=8 n=8
	Exploration familiar vs novel in DBH-Cre mice	vehicle cort	n=9 n=6
	Total exploration times in WT and DBH-Cre mice		n=6-9
S2J	Cort effects on NOR retrieval in Dlx-Cre mice		n=8-11
S2K	Exploration familiar vs novel in WT mice	vehicle cort	n=9 n=8
	Exploration familiar vs novel in Dlx-Cre mice	vehicle cort	n=11 n=9
	Total exploration times in WT and Dlx-Cre mice		n=8-11
S3A	Exploration familiar vs novel in DBH-CB1-KO-control mice	vehicle cort	n=7 n=7
	Exploration familiar vs novel in LC-DBH-CB1-RS mice	vehicle cort	n=8 n=9
	Exploration familiar vs novel in LC-DBH-DN22-CB1-RS mice	vehicle cort	n=9 n=10
	Total exploration times in DBH-CB1-KO-control, LC-DBH-CB1-RS and LC-DBH-DN22-CB1-RS mice		n=7-10
S3B	Exploration familiar vs novel in GABA-CB1-KO-control mice	vehicle cort	n=8 n=8
	Exploration familiar vs novel in HIP-GABA-CB1-RS mice	vehicle cort	n=7 n=7
	Exploration familiar vs novel in HIP-GABA-DN22-CB1-RS mice	vehicle cort	n=7 n=7
	Total exploration times in GABA-CB1-KO-control, HIP-GABA-CB1-RS and HIP-GABA-DN22-CB1-RS mice		n=7-8
S4A	Hippocampal mitochondrial respiration after vehicle or corticosterone treatment		n=10

S4B	Exploration familiar vs novel in WT mice	vehicle cort	n=8 n=6
	Exploration familiar vs novel in DBH-Cre mice (LC-mtsAC-OE)	vehicle cort	n=6 n=6
	Total exploration times in WT and DBH-Cre mice		n=6-8
S4C	Exploration familiar vs novel in WT mice	vehicle cort	n=10 n=10
	Exploration familiar vs novel in Dlx-Cre mice (HIP-mtsAC-OE)	vehicle cort	n=7 n=8
	Total exploration times in WT and Dlx-Cre mice		n=7-10
S4D	Calcium transients amplitude during training session of NOR		n=8
S4E	Exploration familiar vs novel in Dlx-Cre fiber implanted mice	vehicle cort	n=5 n=5
	Total exploration times in fiber implanted mice		n=5
S4F	AKT/Tubulin levels after vehicle or corticosterone (10mg/kg, sc) treatment		n=6
	AKT phosphorylation after vehicle or corticosterone (10mg/kg, sc) treatment		n=5-6
S4G	Effect of MK-2206 pretreatment on cort-induced impairment of NOR consolidation		n=6-7
S4H	Exploration familiar vs novel in mice pretreated with vehicle	vehicle cort	n=6 n=6
	Exploration familiar vs novel in mice pretreated with MK-2206	vehicle cort	n=7 n=7
	Total exploration times		n=6-7
S4I	Effect of MK-2206 pretreatment on cort-induced impairment of NOR retrieval		n=5-7
S4J	Exploration familiar vs novel in mice pretreated with vehicle	vehicle cort	n=6 n=6
	Exploration familiar vs novel in mice pretreated with MK-2206	vehicle cort	n=4 n=7
	Total exploration times		n=4-7
S4K	Exploration familiar vs novel in WT mice	vehicle cort	n=8 n=8
	Exploration familiar vs novel in DBH-Cre mice (LC-MICU-S124A)	vehicle cort	n=9 n=10
	Total exploration times in WT and DBH-Cre mice		n=8-10
S4L	Exploration familiar vs novel in WT mice	vehicle cort	n=9 n=9
	Exploration familiar vs novel in Dlx-Cre mice (HIP-MICU-S124A)	vehicle cort	n=8 n=10
	Total exploration times in WT and Dlx-Cre mice		n=8-10

Is data distribution normal? (Shapiro-Wilk test, alpha=0.05)	Analysis (post-hoc results reported in figures)	Analysis results	P value
yes	One-way ANOVA	F(3,31)=8.585	**P=0.0003**
yes	One-way ANOVA	F(3,29)=7.807	**P=0.0006**
yes	2-way ANOVA (treatment x genotype)	Interaction: F(1,30)=8.382	**P=0.0070**
yes	2-way ANOVA (treatment x genotype)	Interaction: F(1,39)=0.365 Treatment: F(1,39)=81.14 Genotype: F(1,39)=0.007	P=0.5491 **P<0.0001** P=0.9310
yes	2-way ANOVA (treatment x genotype)	Interaction: F(1,43)=0.024 Treatment: F(1, 43)=180.3 Genotype: F(1,43)=0.408	P=0.8773 **P<0.0001** P=0.5264
yes	2-way ANOVA (treatment x genotype)	Interaction: F(1,37)=6.466	**P=0.0153**
yes	2-way ANOVA (treatment x genotype)	Interaction: F (1,36)=25.50	**P<0.0001**
yes	2-way ANOVA (treatment x genotype)	Interaction: F(1,35)=21.14	**P<0.0001**
yes	2-way ANOVA (treatment x genotype)	Interaction: F(1,30)=0.079 Treatment: F(1,30)=39.24 Genotype: F(1,30)=1.093	P=0.7800 **P<0.0001** P=0.3041
yes	2-way ANOVA (treatment x genotype)	Interaction: F(1,46)=36.62	**P<0.0001**
yes	2-way ANOVA (treatment x genotype)	Interaction: F(1,32)=0.014 Treatment: F(1,32)=34.88 Genotype: F(1,32)=0.256	P=0.9064 **P<0.0001** P=0.6163
yes	2-way ANOVA (treatment x genotype)	Interaction: F (1,46)=23.45	**P<0.0001**
no	Kruskall-Wallis	H(3,43)=14.46	**P=0.0023**
no	Kruskall-Wallis	H(5,48)=27.13	**P<0.0001**
yes	2-way ANOVA (treatment x genotype)	Interaction: F(2, 44)=13.80	**P<0.0001**
yes	2-way ANOVA (treatment x genotype)	Interaction: F(2,38)=9.47	**P=0.0005**
yes	2-way ANOVA (treatment x genotype)	Interaction: F(1,22)=0.720 Treatment: F(1,22)=19.69 Genotype: F(1,22)=1.844	P=0.4052 **P=0.0002** P=0.1883
yes	2-way ANOVA (treatment x genotype)	Interaction: F(1,31)=1.79 Treatment: F(1,31)=37.76 Genotype: F(1,28)=3.541	P=0.1897 **P<0.0001** P=0.0703

yes	2-way ANOVA (novelty x treatment)	Interaction: F(1,16)=5.083	**P=0.0385**
yes	Two-tailed unpaired t-test	t(8)= 5.644	**P=0.0005**
non applicable	Pearson's correlation	R2=0.3900	P=0.0536
yes	2-way ANOVA (treatment x genotype)	Interaction :F(1,31)= 4.216	**P=0.0486**
yes	2-way ANOVA (treatment x genotype)	Interaction: F(1,31)=7.965	**P=0.0083**

yes no yes yes	Paired t-test/ Wilcoxon test	t=9.323, df=10 t=2.497, df=7 t=0.9479, df=9	**P<0.0001** **P=0.0156** **P=0.0412** P=0.3680
no	Kruskall-Wallis	H(4,35)=5.064	P=0.1685
yes yes no no	Paired t-test/ Wilcoxon test	t=8.504, df=10 t=9.701, df=5	**P<0.0001** **P=0.0002** **P=0.0391** P=0.3828
no	Kruskall-Wallis	H(4,33)=2.441	P=0.4861
yes	Unpaired t-test	t=0.1263, df=12	P=0.9016
yes	Welsh One way ANOVA	W(2,9.8)= 39.72	**P<0.0001**
yes	Unpaired t-test	t (21) =2.254	**P=0.0350**
yes	Unpaired t-test	t (21) =0.981	P=0.3377
yes yes	Paired t-test	t=14.29, df=9 t=1.303, df=8	**P<0.0001** P=0.2288
yes yes	Paired t-test	t=9.557, df=7 t=7.384, df=6	**P<0.0001** **P=0.0003**
yes	2-way ANOVA (treatment x genotype)	Interaction: F(1,31)=2.309 Treatment: F(1,31)=2.036 Genotype: F(1,31)=0.8593	P=0.1388 P=0.1637 P=0.3611
no yes	Paired t-test/ Wilcoxon test	 t=1.052, df=11	**P=0.0001** P=0.3152
yes yes	Paired t-test	t=5.752, df=8 t=1.301, df=7	**P=0.0004** P=0.2345
yes	2-way ANOVA (treatment x genotype)	Interaction: F(1,39)=0.959 Treatment: F(1,39)=0.03 Genotype: F(1,39)=12.11	P=0.3334 P=0.8627 **P=0.0012**
yes yes	Paired t-test	t=14.44, df=9 t=1.664, df=12	**P<0.0001** P=0.1220
no no	Wilcoxon test		**P=0.0001** P>0.9999

yes	2-way ANOVA (treatment x genotype)	Interaction: F(1,36)=0.102 Treatment: F(1, 36)=0.055 Genotype: F(1,36)=6.076	P=0.7508 P=0.8160 **P=0.0186**
yes yes	Paired t-test	t=9.593, df=10 t=0.9760, df=10	**P<0.0001** P=0.3521
yes no	Paired t-test/ Wilcoxon test	t=10.38, df=8	**P<0.0001** **P=0.0020**
no	Kruskall-Wallis	H(4,42)=4.753	P=0.1908
yes yes	Paired t-test	t=16.01, df=12 t=1.887, df=10	**P<0.0001** P=0.0885
yes yes	Paired t-test	t=12.76, df=7 t=5.396, df=7	**P<0.0001** **P=0.0010**
yes	2-way ANOVA (treatment x genotype)	Interaction: F(1,36)=0.914 Treatment: F(1,36)=0.144 Genotype: F(1,36)=2.411	P=0.3452 P=0.7067 P=0.1292
yes yes	Paired t-test	t=12.21, df=10 t=1.100, df=9	**P<0.0001** P=0.2998
yes yes	Paired t-test	t=8.873, df=10 t=3.471, df=6	**P<0.0001** **P=0.0133**
yes	2-way ANOVA (treatment x genotype)	Interaction: F(1,31)=2.650 Treatment: F(1,31)=5.080 Genotype: F(1,31)=0.466	P=0.1137 P=0.0614 P=0.5001
yes no	Paired t-test/ Wilcoxon test	t=7.663, df=6	**P=0.0003** P=0.9375
yes no	Paired t-test/ Wilcoxon test	t=5.333, df=7	**P=0.0011** P=0.9102
yes	2-way ANOVA (treatment x genotype)	Interaction: F(1,30)=0.394 Treatment: F(1,30)=2.233 Genotype: F(1,30)=22.39	P=0.5347 P=0.1455 **P<0.0001**
no yes	Paired t-test/ Wilcoxon test	t=0.08345, df=11	**P<0.0001** P=0.9350
yes yes	Paired t-test	t=6.914, df=11 t=8.349, df=10	**P<0.0001** **P<0.0001**
no	Kruskall-Wallis	H(4,50)=22.89	**P<0.0001**
yes yes	Paired t-test	t=11.07, df=7 t=0.5544, df=9	**P<0.0001** P=0.5928
no yes	Paired t-test/ Wilcoxon test	t=1.271, df=8	**P=0.0039** P=0.2393
yes	2-way ANOVA (treatment x genotype)	Interaction: F(1,32)=0.264 Treatment: F(1,32)=0.578 Genotype: F(1,32)=0.529	P=0.6110 P=0.4527 P=0.4722
yes yes	Paired t-test	t=6.685, df=6 t=1.061, df=7	**P=0.0005** P=0.3238
yes yes	Paired t-test	t=10.77, df=12 t=8.407, df=12	**P<0.0001** **P<0.0001**
no	Kruskall-Wallis	H(4,42)=1.72	P=0.6304
yes yes	Paired t-test	t=6.247, df=11 t=1.995, df=11	**P<0.0001** P=0.0714

yes yes	Paired t-test	t=7.810, df=9 t=6.146, df=9	**P<0.0001** **P=0.0002**
no	Kruskall-Wallis	H(4,44)=9.606	**P=0.0222**
yes yes	Paired t-test	t=5.445, df=10 t=9.629, df=10	**P=0.0003** **P<0.0001**
yes yes	Paired t-test	t=7.196, df=4 t=1.894, df=5	**P=0.0020** P=0.1168
no no	Wilcoxon test		**P=0.0078** P=0.4844
yes	2-way ANOVA (treatment x genotype)	Interaction: F(2,42)=1.479 Treatment: F(1,42)=3.817 Genotype: F(2,42)=24.35	P=0.2394 P=0.0574 **P<0.0001**
yes	2-way ANOVA (treatment x genotype)	Interaction: F(1,26)=0.086 Treatment: F(1,26)=43.50	P=0.3613 **P<0.0001**
no yes	Paired t-test/ Wilcoxon test	t=1.035, df=7	**P=0.0078** P=0.3352
yes yes	Paired t-test	t=6.472, df=8 t=0.03923, df=5	**P=0.0002** P=0.9702
yes	2-way ANOVA (treatment x genotype)	Interaction: F(1,27)=0.108 Treatment: F(1,27)=1.897 Genotype: F(1,27)=0.024	P=0.7453 P=0.1797 P=0.8776
no	Kruskall-Wallis	H(3,36)=17.50	**P=0.0006**
no yes	Paired t-test/ Wilcoxon test	t=0.06399, df=7	**P=0.0078** P=0.9508
yes yes	Paired t-test	t=6.768, df=10 t=1.455, df=8	**P<0.0001** P=0.1838
yes	2-way ANOVA (treatment x genotype)	Interaction: F(1,33)=0.014 Treatment: F(1, 33)=1.454 Genotype: F(1,33)=0.287	P=0.9069 P=0.2365 P=0.5952
yes yes	Paired t-test	t=9.239, df=6 t=9.833, df=6	**P<0.0001** **P<0.0001**
no yes	Paired t-test/ Wilcoxon test	t=0.07299, df=8	**P=0.0078** P=0.9436
yes yes	Paired t-test	t=5.779, df=8 t=7.453, df=9	**P=0.0004** **P<0.0001**
no	Kruskall-Wallis	H(6,50)=12.15	**P=0.0328**
yes yes	Paired t-test	t=5.570, df=7 t=7.079, df=7	**P=0.0008** **P=0.0002**
yes yes	Paired t-test	t=9.200, df=6 t=0.569, df=6	**P<0.0001** P=0.5900
yes yes	Paired t-test	t=7.487, df=6 t=5.274, df=6	**P=0.0003** **P=0.0019**
yes	2-way ANOVA (treatment x genotype)	Interaction: F(2,38)=0.569 Treatment: F(1, 38)=7.682 Genotype: F(2,38)=4.013	P=0.5706 P=0.9931 **P=0.0262**
yes	2-way ANOVA (treatment x time)	Interaction: F(1,18)=0.184 Treatment: F(1,18)=0.008 Time: F(1,18)=0.4558	P=0.6731 P=0.9276 P=0.5082

yes no	Paired t-test/ Wilcoxon test	t=4.047, df=7	**P=0.0049** P=0.8438
yes yes	Paired t-test	t=4.087, df=5 t=0.5358, df=5	**P=0.0002** P=0.6151
yes	2-way ANOVA (treatment x genotype)	Interaction: F(1,22)=0.626 Treatment: F(1,22)=0.099 Genotype: F(1,22)=0.003	P=0.4372 P=0.7561 P=0.9533
yes yes	Paired t-test	t=8.008, df=9 t=1.043, df=9	**P<0.0001** P=0.3243
yes yes	Paired t-test	t=3.850, df=6 t=4.737, df=7	**P=0.0085** **P=0.0210**
yes	2-way ANOVA (treatment x genotype)	Interaction: F(1,28)=1.462 Treatment: F(1,28)=0.102 Genotype: F(1,28)=0.256	P=0.2367 P=0.7518 P=0.6166
yes	Paired t-test	t= 0.1802 df=7	P=0.8621
yes yes	Paired t-test	t=4.000, df=4 t=0.6263, df=4	**P=0.0161** P=0.5651
yes	Unpaired t-test	t=0.7029, df=8	P=0.5021
yes	Unpaired t-test	t=0.1277, df=10	P=0.9009
yes	Unpaired t-test	t=2.805, df=9	**P=0.0205**
no	Kruskall-Wallis test	H(4,26)=10.6	**P=0.0141**
yes yes	Paired t-test	t=3.770, df=5 t=0.5703, df=5	**P=0.0130** P=0.5931
yes yes	Paired t-test	t=4.746, df=6 t=7.296, df=6	**P=0.0032** **P=0.0003**
yes	2-way ANOVA (pretreatment x treatment)	Interaction: F(1,22)=0.37 Pretreatment: F(1,22)=0.2 Treatment: F(1,22)=0.001	P=0.5458 P=0.6780 P=0.9900
no	Kruskall-Wallis test	H(4,24)=12.53	**P=0.0073**
yes yes	Paired t-test	t=6.501, df=5 t=0.8818, df=5	**P=0.0013** P=0.4183
no yes	Paired t-test/ Wilcoxon test	t=5.503, df=6	P=0.0581 **P=0.0015**
yes	2-way ANOVA (pretreatment x treatment)	Interaction: F(1,19)=0.15 Pretreatment: F(1,19)=0.1 Treatment: F(1,19)=1.13	P=0.7072 P=0.7489 P=0.3008
yes yes	Paired t-test	t=5.990, df=7 t=0.7324, df=7	**P=0.0005** P=0.4877
no yes	Paired t-test/ Wilcoxon test	t=3.951, df=8	**P=0.0020** **P=0.0042**
no	Kruskall-Wallis test	H(4,35)=3.281	P=0.3503
yes yes	Paired t-test	t=7.592, df=8 t=1.140, df=8	**P<0.0001** P=0.2874
no yes	Paired t-test/ Wilcoxon test	t=3.954, df=8	**P=0.0078** **P=0.0042**
no	Kruskall-Wallis test	H(4,25)=1.381	P=0.7100

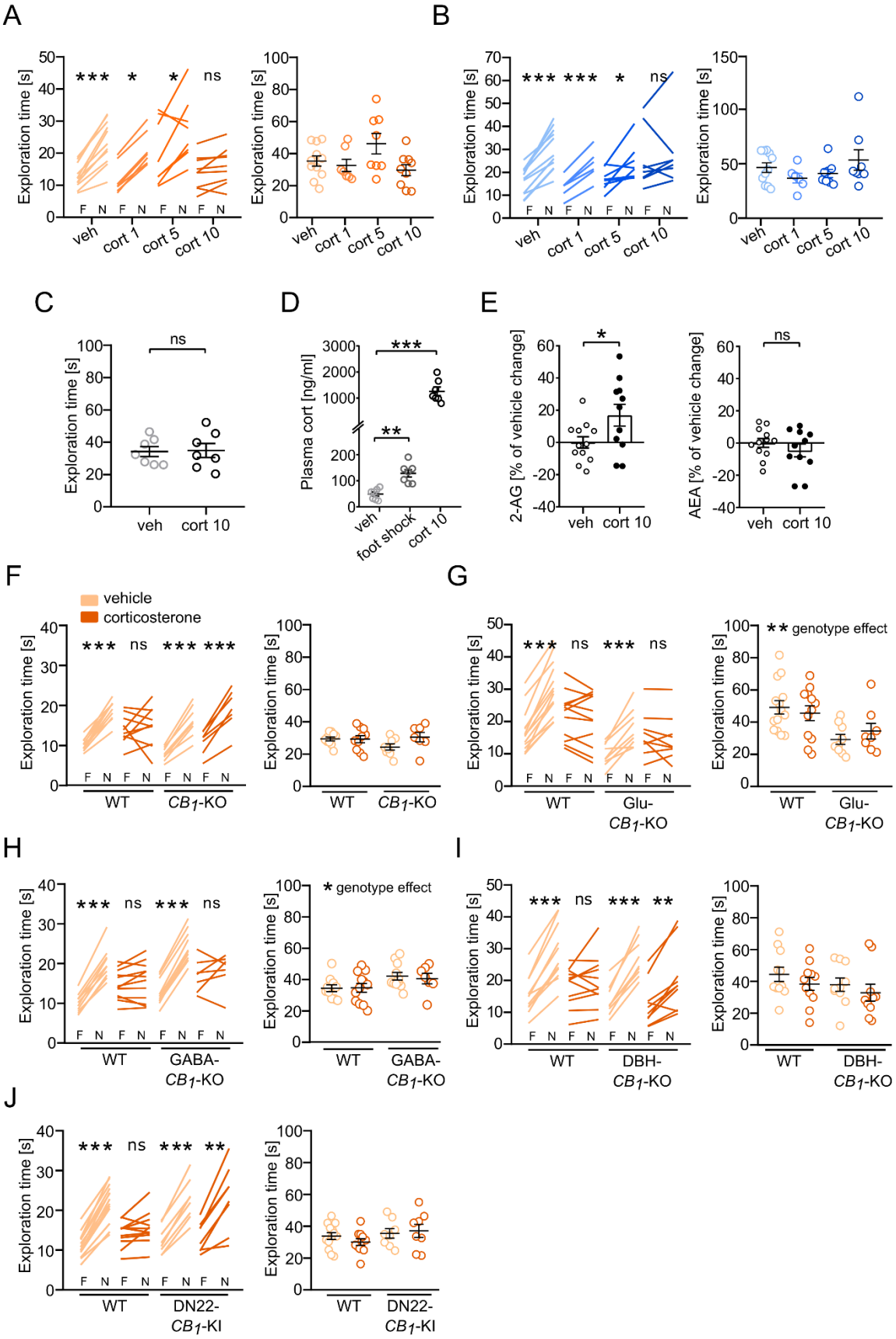
A
B
C
D
E
F
G
H
I
J
Exploration time [s]
veh
cort 1
cort 5
cort 10
Plasma cort [ng/ml]
foot shock
2-AG [% of vehicle change]
AEA [% of vehicle change]
vehicle
corticosterone
WT
CB1-KO
Glu-CB1-KO
GABA-CB1-KO
DBH-CB1-KO
DN22-CB1-KI
genotype effect

Figure S1. Effects of corticosterone injection on plasma corticosterone levels, hippocampal endocannabinoid levels and exploratory behavior at different stages of NOR task. Related to Figure 1.

(**A**) Exploration times of familiar ("F") and novel ("N") objects (left panel) and total exploration times (right panel) after vehicle or corticosterone (1-10 mg/kg) treatment during NOR consolidation in WT mice.

(**B**) Exploration times of familiar ("F") and novel ("N") objects (left panel) and total exploration times (right panel) after vehicle or corticosterone (1-10 mg/kg) treatment before NOR retrieval in WT mice.

(**C**) Exploration times of novel identical objects presented during training phase of NOR task in WT mice 30 minutes after injection of vehicle or corticosterone (10 mg/kg, sc).

(**D**) Plasma corticosterone levels 30 min after vehicle, single foot shock (2s, 0.5 mA) or 10 mg/kg (sc) corticosterone administration in WT mice.

(**E**) Hippocampal 2-AG (left panel), but not AEA (right panel) levels were elevated 30 min after corticosterone (10 mg/kg, sc) administration in WT mice.

(**F-J**) Exploration times of familiar ("F") and novel ("N") objects (left panels) and total exploration times (right panels) after vehicle or corticosterone treatment during NOR consolidation in full *CB$_1$*-KO mice (**F**), Glu-*CB$_1$*-KO mice (**G**), GABA-*CB$_1$*-KO mice (**H**), DBH-*CB$_1$*-KO mice (**I**) or DN22-*CB$_1$*-KI mice (**J**) and their respective WT littermates.

Significant differences marked with *p<0.05, **p<0.01, ***p < 0.001; ns- not significant. Data presented as mean ± SEM. Statistical tests and numbers of animals used are described in Table S1.

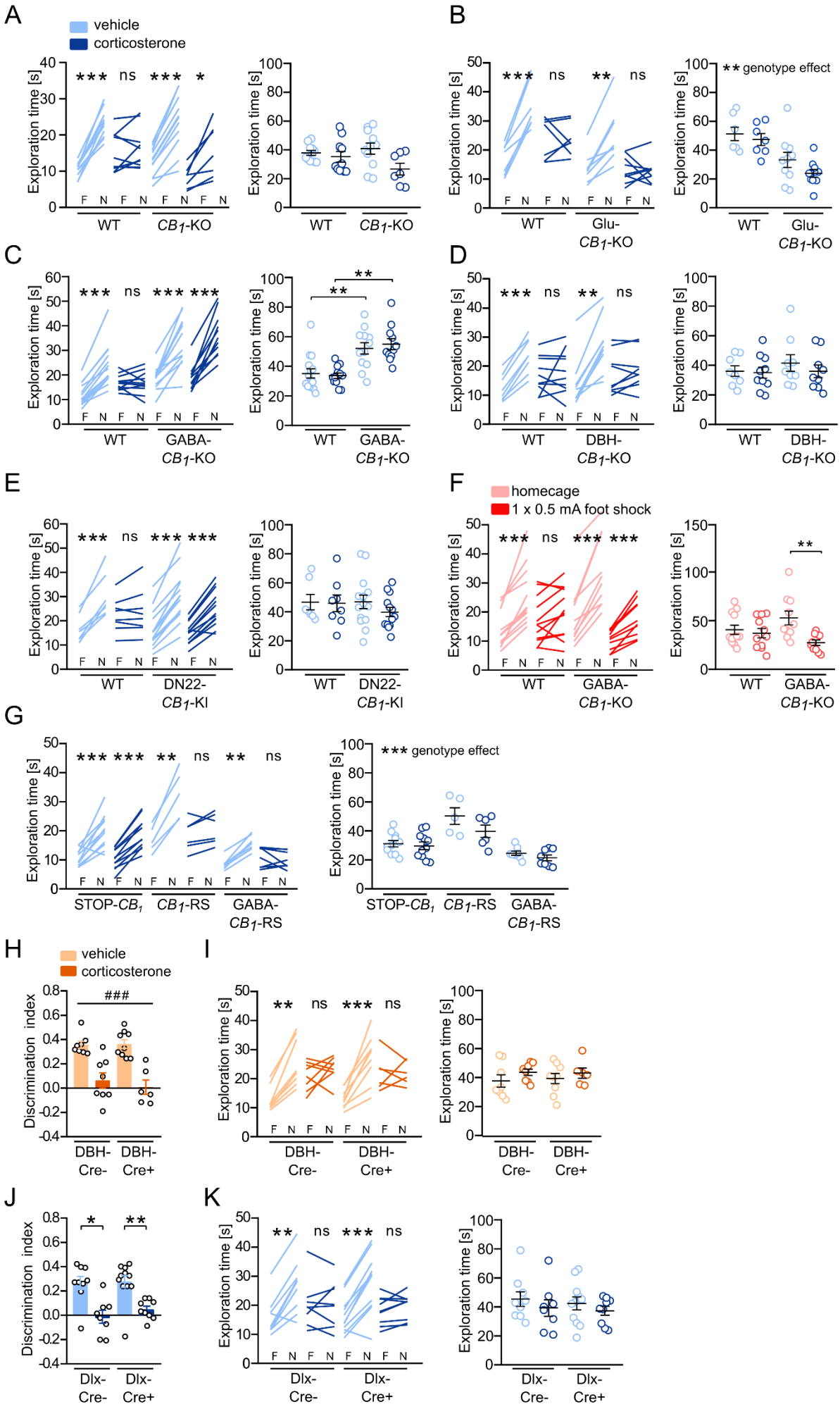
A
vehicle
corticosterone
Exploration time [s]
*** ns *** *
F N F N F N F N
WT
CB1-KO
** genotype effect
B
*** ns ** ns
Glu-CB1-KO
C
*** ns *** ***
**
GABA-CB1-KO
D
DBH-CB1-KO
E
DN22-CB1-KI
F
homecage
1 x 0.5 mA foot shock
G
*** ** ns
STOP-CB1
CB1-RS
GABA-CB1-RS
*** genotype effect
H
Discrimination index
###
DBH-Cre-
DBH-Cre+
I
J
*
Dlx-Cre-
Dlx-Cre+
K

Figure S2. Effects of corticosterone injection or foot shock stress on exploratory behavior at different stages of NOR task. Related to Figure 1.

(**A-E**) Exploration times of familiar ("F") and novel ("N") objects (left panels) and total exploration times (right panels) after vehicle or corticosterone treatment before NOR retrieval in full *CB$_1$*-KO mice (**A**), Glu-*CB$_1$*-KO mice (**B**), GABA-*CB$_1$*-KO mice (**C**), DBH-*CB$_1$*-KO mice (**D**) or DN22-*CB$_1$*-KI mice (**E**) and their respective WT littermates.

(**F**) Times of exploration of familiar ("F") and novel ("N") objects (left panel) and total exploration times (right panel) after single 0.5 mA foot shock stress applied before NOR retrieval in WT and GABA-*CB$_1$*-KO mice.

(**G**) Exploration times of familiar ("F") and novel ("N") objects (left panel) and total exploration times (right panel) after vehicle or corticosterone treatment before NOR retrieval in STOP-*CB$_1$* mice, *CB$_1$*-RS mice and GABA-*CB$_1$*-RS mice.

(**H-K**) Presence of Cre in noradrenergic or GABAergic cells does not contribute to NOR-impairing effects of corticosterone during consolidation (**H,I**) nor retrieval (**J,K**).

Significant differences marked with *p<0.05, **p<0.01, ***p < 0.001; ns- not significant. Data presented as mean ± SEM. Statistical tests and numbers of animals used are described in Table S1.

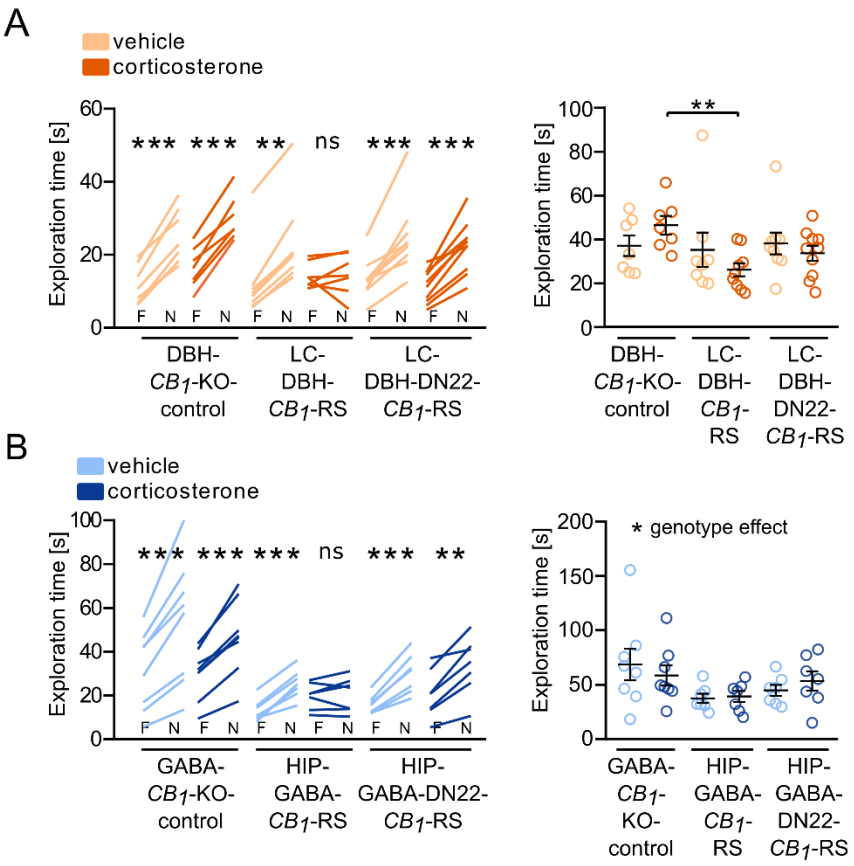

Figure S3. Effects of corticosterone injection on exploratory behavior at different stages of NOR task. Related to Figure 2.

(**A**) Exploration times of familiar ("F") and novel ("N") objects (left panel) and total exploration times (right panel) after vehicle or corticosterone treatment during NOR consolidation in DBH-*CB*$_1$-KO mice injected with control virus (DBH-*CB*$_1$-KO-control), LC-DBH-*CB*$_1$-RS mice and LC-DBH-DN22-*CB*$_1$-RS mice.

(**B**) Times of exploration of familiar ("F") and novel ("N") objects (left panel) and total exploration times (right panel) after vehicle or corticosterone treatment before NOR retrieval in GABA-*CB*$_1$-KO mice injected with control virus (GABA-*CB*$_1$-KO-control), HIP-GABA-*CB*$_1$-RS mice and HIP-GABA-DN22-*CB*$_1$-RS mice.

Significant differences marked with *p<0.05, **p<0.01, ***p < 0.001; ns- not significant. Data presented as mean ± SEM. Statistical tests and numbers of animals used are described in Table S1.

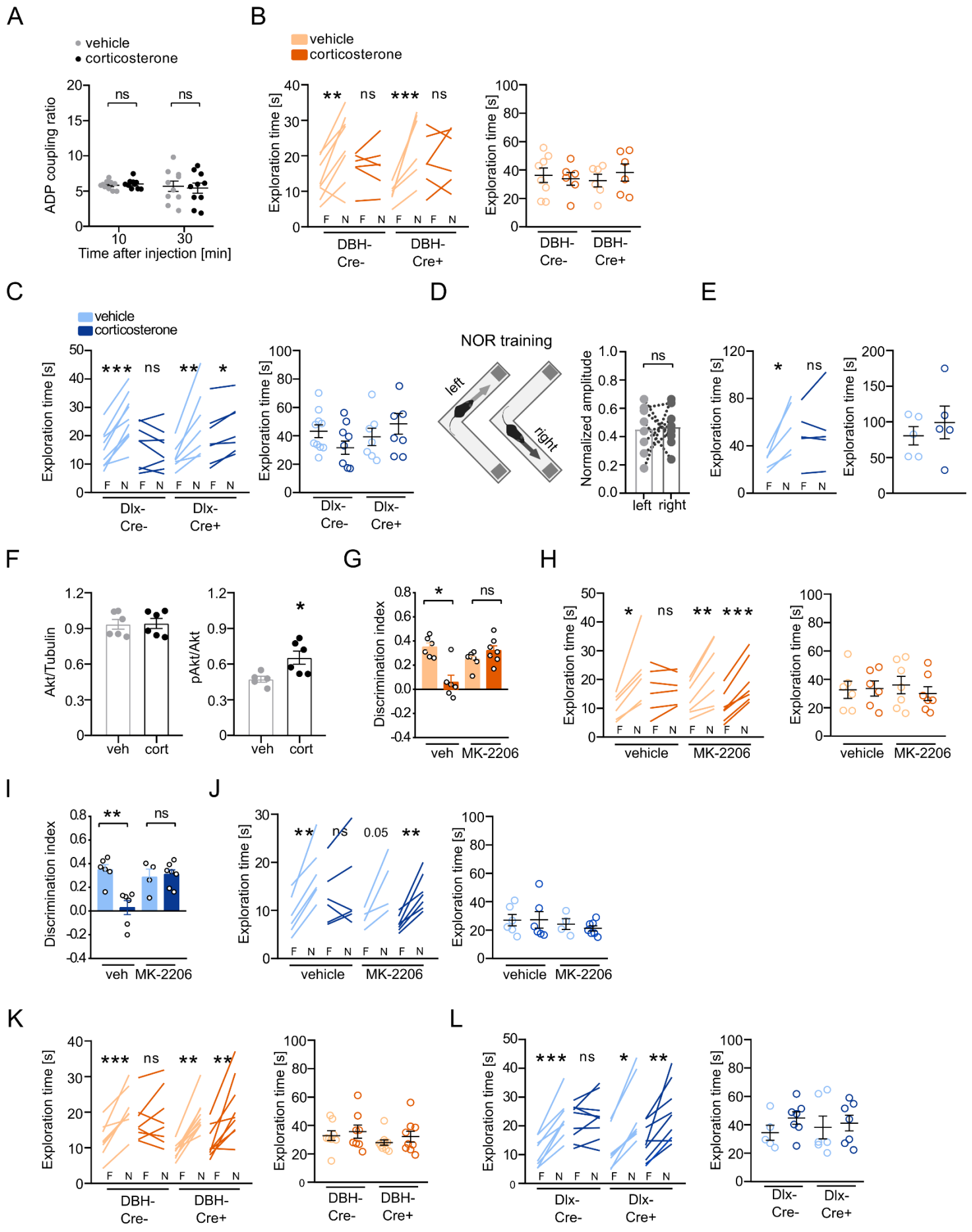
A
vehicle
corticosterone
ADP coupling ratio
ns
ns
10
30
Time after injection [min]
B
vehicle
corticosterone
Exploration time [s]
**
ns
***
ns
F N F N F N F N
DBH- Cre-
DBH- Cre+
C
vehicle
corticosterone
***
ns
**
*
Dlx- Cre-
Dlx- Cre+
D
NOR training
left
right
Normalized amplitude
ns
left right
E
*
ns
F N F N
F
Akt/Tubulin
pAkt/Akt
veh
cort
G
Discrimination index
*
ns
veh
MK-2206
H
*
ns
**
***
vehicle
MK-2206
I
Discrimination index
**
ns
veh
MK-2206
J
**
ns
0.05
**
vehicle
MK-2206
K
***
ns
**
**
DBH- Cre-
DBH- Cre+
L
***
ns
*
**
Dlx- Cre-
Dlx- Cre+

Figure S4. Effects of corticosterone injection on hippocampal mitochondrial respiration, Akt phosphorylation, and exploratory behavior at different stages of NOR task. Related to Figure 3.

(**A**) ADP-induced complex I-dependent hippocampal mitochondrial respiration 10 and 30 minutes after vehicle or 10 mg/kg corticosterone administration.

(**B, C**) Exploration times of familiar ("F") and novel ("N") objects (left panels) and total exploration times (right panels) after vehicle or corticosterone treatment during NOR consolidation (**B**) or retrieval (**C**) in control mice and mice overexpressing mt-sAC in the LC noradrenergic neurons or hippocampal GABA-ergic cells, respectively.

(**D**) Calcium transients amplitude is similar during the approach towards each of the two identical objects presented during training session of NOR.

(**E**) Exploration times of familiar ("F") and novel ("N") objects (left panel) and total exploration times (right panel) after vehicle or corticosterone treatment before NOR retrieval in animals that underwent fiber photometry experiment.

(**F**) The effect of 10 mg/kg corticosterone injection (sc) on Akt phosphorylation in the hippocampus. Densitometric analysis of western blot results. Akt signal was normalized on Tubulin (left); Akt phosphorylation expressed as pAkt/Akt ratio (right).

(**G-J**) The Akt blocker MK-2206 blocked corticosterone-induced impairment of both NOR consolidation (**G**) and retrieval (**I**). Exploration times of familiar ("F") and novel ("N") objects (left panels) and total exploration times (right panels) after vehicle or corticosterone treatment during NOR consolidation (**H**) or retrieval (**J**) in mice pretreated with Akt blocker, MK-2206.

(**K,L**) Exploration times of familiar ("F") and novel ("N") objects (left panels) and total exploration times (right panels) after vehicle or corticosterone treatment during NOR consolidation (**K**) or retrieval (**L**) in mice expressing non- phosphorylatable form of MICU in the LC of DBH-Cre mice or in the HIP of Dlx-Cre+ mice, respectively.

Significant differences marked with *p<0.05, **p<0.01, ***p < 0.001; ns- not significant. Data presented as mean ± SEM. Statistical tests and numbers of animals used are described in Table S1.